Accepted Manuscript

Optimization of physicochemical properties for 4-anilinoquinazoline inhibitors of trypanosome proliferation

Jennifer L. Woodring, Kelly A. Bachovchin, Kimberly G. Brady, Mitchell F. Gallerstein, Jessey Erath, Scott Tanghe, Susan E. Leed, Ana Rodriguez, Kojo Mensa-Wilmot, Richard J. Sciotti, Michael P. Pollastri

PII: S0223-5234(17)30799-7

DOI: 10.1016/j.ejmech.2017.10.007

Reference: EJMECH 9799

To appear in: *European Journal of Medicinal Chemistry*

Received Date: 13 April 2017

Revised Date: 1 October 2017

Accepted Date: 3 October 2017

Please cite this article as: J.L. Woodring, K.A. Bachovchin, K.G. Brady, M.F. Gallerstein, J. Erath, S. Tanghe, S.E. Leed, A. Rodriguez, K. Mensa-Wilmot, R.J. Sciotti, M.P. Pollastri, Optimization of physicochemical properties for 4-anilinoquinazoline inhibitors of trypanosome proliferation, *European Journal of Medicinal Chemistry* (2017), doi: 10.1016/j.ejmech.2017.10.007.

TABLE OF CONTENTS GRAPHIC

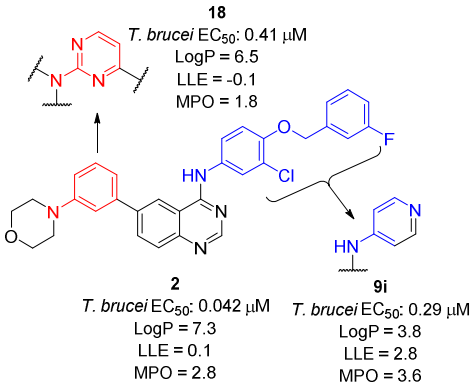

Optimization of Physicochemical Properties for 4-Anilinoquinazoline Inhibitors of Trypanosome Proliferation

Jennifer L. Woodring,[a] Kelly A. Bachovchin,[a] Kimberly G. Brady,[a] Mitchell F. Gallerstein,[a] Jessey Erath,[b] Scott Tanghe,[b] Susan E. Leed,[c] Ana Rodriguez,[b,e] Kojo Mensa-Wilmot,[d] Richard J. Sciotti,[c] and Michael P. Pollastri.*[a]

[a]*Northeastern University Department of Chemistry & Chemical Biology, 360 Huntington Avenue, Boston, MA 02115 USA. Tel: 617-373-2703; E-mail: m.pollastri@neu.edu*

[b]*New York University School of Medicine, Department of Microbiology, Division of Parasitology, 341 E. 25th St. New York, NY 10016 USA*

[c]*Experimental Therapeutics, Walter Reed Army Institute for Research,2460 Linden Lane, Silver Spring, MD, 20910*

[d]*University of Georgia Department of Cellular Biology, Athens, GA USA*

[e]*Anti-Infectives Screening Core, New York University School of Medicine, New York, NY 10010*

Abstract

Human African trypanosomiasis (HAT) is a deadly disease in need of new chemotherapeutics that can cross into the central nervous system. We previously reported the discovery of **2** (NEU-617), a small molecule with activity against *T. brucei* bloodstream proliferation. Further optimization of **2** to improve the physicochemical properties (LogP, LLE,[1] and MPO score)[2] have led us to twelve sub-micromolar compounds, most importantly

the headgroup variants **9i** and **9j**, and the linker variant **18**. Although these 3 compounds had reduced potency compared to **2**, they all had improved LogP, LLE and MPO scores. Cross-screening these analogs against other protozoan parasites uncovered **9o** with potent activity towards *T. brucei*, *T. cruzi* and *L. major*, while four others compounds (**17**, **18**, **21**, **26**) showed activity towards *P. falciparum* D6. This reinforces the effectiveness of lead repurposing for the discovery of new protozoan disease therapeutics.

Keywords

Neglected tropical disease, human African trypanosomiasis, target class repurposing, *Trypanosoma brucei*, *Leishmania major*, *Trypanosoma cruzi*, *Plasmodium falciparum.*

1. Introduction

Human African trypanosomiasis (HAT) is a neglected tropical disease endemic in 36 countries of sub-Saharan Africa. The parasitic causative agent, *Trypanosoma brucei*, puts 65 million people at risk and is fatal if not treated. Current treatments for HAT are limited, requiring administration by intramuscular or intravenous injection. Clinics needed to treat patients are not easily accessible in the rural regions of Africa where HAT is endemic [3]. In addition, vaccines are not available to prevent infection. As a result, new drugs are needed to control and eradicate this disease.

Lead repurposing is the method of utilizing, as a starting point, well-established classes of small molecules known for their efficacy against human targets with homologous function in parasites, and re-optimizing the compounds for desired properties and anti-parasitic activity [4].

Our previous lead repurposing work has primarily focused on inhibitors of phosphodiesterases[5-10] and protein kinases [11-16].

We previously reported that the human tyrosine kinase inhibitor lapatinib (**1**), shown in **Figure 1**, prevents proliferation of bloodstream *T. brucei* with an EC_{50} of 1.54 µM [17, 18]. Further optimization studies, especially the "tail" region (in red), led to the discovery of **2** (NEU-617), with a potency of 0.042 µM and improved parasite selectivity over **1** [12].

Figure 1 – Discovery of **2**, and paths towards the optimization of physicochemical properties.

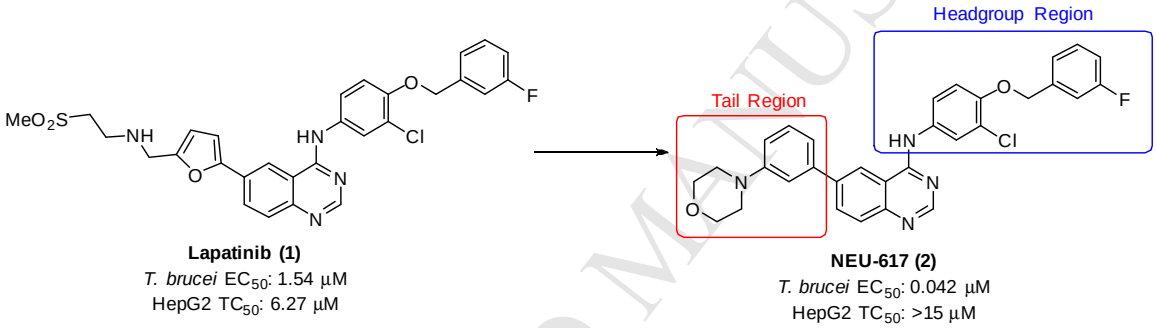

Despite its excellent potency and selectivity, the physicochemical properties of **2** need improvement to convert it into a lead drug (*i.e.*, capable of reducing parasitemia 100-fold in a mouse model of HAT) [18-20]. For example, **2** is highly lipophilic (LogP = 7.3), has high molecular weight (541), and has low lipophilic ligand efficiency (LLE = 0.1) [1]. Entering the central nervous system (CNS) is a requirement for treating stage 2 HAT, as trypanosomes have crossed the blood-brain barrier. A multiple parameter optimization (MPO) score incorporates several key physicochemical properties (molecular weight, LogP, hydrogen bond donors, polar surface area, and pKa) in gauging the possibility of drugs crossing the blood-brain barrier. A higher MPO score ranging from 4.0-6.0 suggests a compound is more likely to be brain penetrant

[2]. With an MPO score of 2.8, compound **2** is predicted to be a poor CNS drug candidate, and this was further confirmed by mouse pharmacokinetics experiments that were previously reported [21]. To resolve the issues that we identified in **2**, optimization efforts focused specifically on the "headgroup" region (in blue in **Figure 1**) and the "tail" region (in red in **Figure 1**).

2. Results & Discussion

In the same report for the discovery of **2**, we observed an enhanced potency by truncating the headgroup of lapatinib-related analogs. For example, the truncated analog **4** (in blue in **Figure 2**) had a 1.7-fold increase in potency and improved MPO and cLogP values over the lapatinib-like headgroup in compound **3** [12]. Furthermore, the analysis of **5** (NEU-964) shows the removal of the sulfonyl group, in line with the tail of **2** (in red in **Figure 2**), was more potent than its predecessor **4**, albeit not as potent as **2**. This led to the hypothesis that a reduction in size of the headgroup on **2**, by replacing the aniline moiety with aminoheterocycles, could provide potent analogs that inhibit trypanosome proliferation while potentially improving MPO scores and LLE values.

Figure 2 – Progression of headgroup truncation as a means of improving potency and physicochemical properties

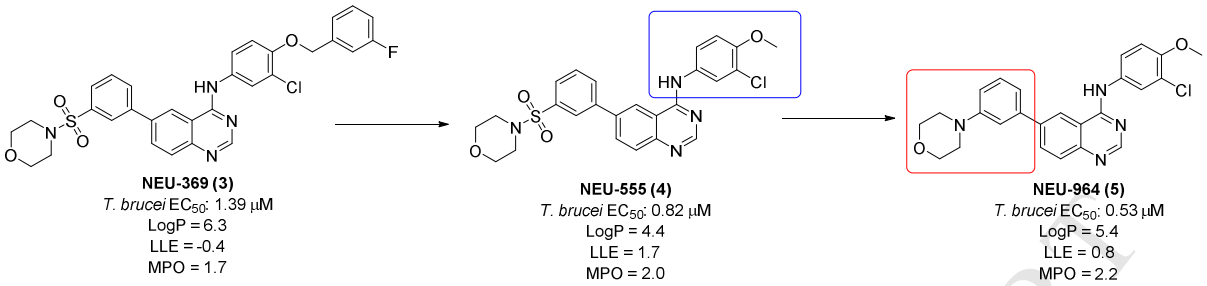

To achieve our goals, we enumerated a virtual library (VL) *in silico* using 247 commercially available aromatic amines. We then prioritized the compounds by performing shape and electrostatics similarity comparison to the headgroup of **2** using ROCS and EON (OpenEye Scientific Software) and Kpμμ predictive blood-brain barrier partitioning (predictions provided by AstraZeneca) [22]. After removal of products with an ET_Combo score <1 (meaning lack of shape/electrostatic similarity and undesirable Kpμμ), 121 remaining compounds were filtered by limiting cLogP <3 and TPSA between 60-130 Å. This provided an initial set of nine prioritized compounds for synthesis (see **Table S.1** for library parameters). In addition to the nine compounds, we also prepared analogs that walked the nitrogen atom(s) around the heterocyclic ring to include all positional isomers of the pyridines, pyrimidines, pyridazines, and pyrazines. We noted that the nine compounds from the original VL contained only six-membered heteroaromatic head groups. Therefore, to round out the set, we added five-membered heteroaromatic rings (pyrazoles, oxazoles, thiazoles, thiazines) and their commercially available isomers. This established a complete library comprised of 26 analogs.

Synthesis of these new compounds proved surprisingly challenging when employing the sequence we reported for preparation of **2** [12]. A new approach was therefore established as shown in **Scheme 1**. Optimized Suzuki chemistry resulted in improved results with employment

of Pd(dppf)Cl_2-DCM, rather than $Pd(PPh_3)_4$ to afford the desired intermediate **7** in moderate yields. To prepare chloroquinazoline **8**, we applied modified Appel conditions [23] which proved more reliable in this case than thionyl chloride as previously reported. *In lieu* of standard SN_{AR} conditions (which showed irreproducible results) we utilized a modified Buchwald-Hartwig coupling for aryl chlorides [24-26] for the installation of the headgroup to obtain compounds **9a-x**. Production of analogs utilizing nucleotide derivatives like cytosine required another set of reaction conditions, utilizing K_2CO_3 and acetone with microwave irradiation to produce **10a-b**.

Scheme 1. Preparation of headgroup replacement analogs **9** and **10**.

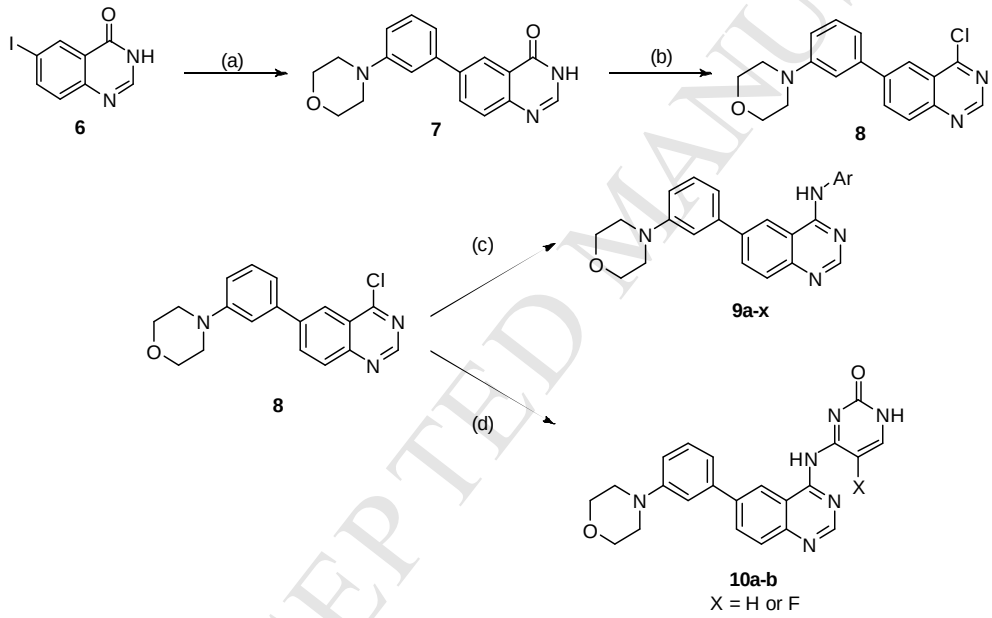

Reagents and Conditions: (a) 4-(3-(4,4,5,5-tetramethyl-1,3,2-dioxaborolan-2-yl)phenyl)morpholine, 2M Na_2CO_3 in H_2O, Pd(dppf)Cl_2-DCM, DME/EtOH (3:2), 85^{o}C, 6 h, 66%; (b) PPh_3, CCl_4, DCE, N_2, 70^{o}C, 12 h, 97%; (c) Ar-NH_2, K_2CO_3, xantphos, $Pd(OAc)_2$, 1,4-dioxane, N_2, 105^{o}C, 12 h, 5-78%; (d) Ar-NH_2, K_2CO_3, acetone, N_2, MW, 120^{o}C, 1 h, 5-23%

The biological data for the resulting headgroup replacement library is presented in **Table 1**. Of the 26 compounds tested, nine had sub-micromolar potency against *T. brucei*. The most potent were pyridine (**9i**, EC_{50} = 0.29 µM) and pyrimidine-substituted products (**9j**, EC_{50} = 0.32 µM). The isomers of the pyridines (**9h, i, q**) have activities within a ten-fold window ranging from 0.29 µM to 2.1 µM. The pyrimidine isomers (**9b, j, l**) have a wider potency range from 0.32 µM to 7.0 µM. There seems to be no significant importance or pattern to the nitrogen atom positioning, based on comparison of the pyridyl and pyrimidinyl data. Interestingly, methylation of the 1,3-amino pyrimidine resulted in a three-fold loss of potency (**9k**, 1.0 µM) when compared to **9j**, and little difference was observed between the free amine **9t** and the corresponding acetamide **9r**.

In addition, the thiazoles (**9u, v, x**), thiazine (**9w**), and oxazoles (**9o-p**) also showed roughly equivalent potency with each other, within ~two-fold range. Overall, the triazines (**9c**, **d**), pyrazole (**9a**), pyridazines (**9e**, **f**, **m**), pyrazines (**9g**, **s**), and cytosine derivatives (**10a-b**) were not highly active against *T. brucei*. However, we note that the fluorinated cytosine (**10b**) showed a significant (>50-fold) increase in potency compared to **10a**.

Despite none of these compounds having improved potency over **2**, and both pyridine **9i** and pyrimidine **9j** were the only compounds with improved potency over the truncated **5** (NEU-964), every compound had a significant improvement in lipophilicity (between 2-5 orders of magnitude) and MPO score (between 1.5-3 orders of magnitude). **Figure 3** clearly shows these 26 analogs (in red) had significantly improved physicochemical properties, with higher MPO scores and lower LogP values, over the compounds that were simultaneously reported in the SAR and discovery of **2** (orange) [12]. Accordingly, we observed an improvement in LLE from

0.1 (for **2**) to as high as 3.2 (for **10b**). In fact, the only compound to not have an improved LLE from this library was compound **10a** due to its inactivity in the assay.

Figure 3 – Representation of the improvements in physicochemical properties for the compounds in the headgroup library (red) and linker/tail library (blue) over the compounds used in the SAR of **2** (orange)

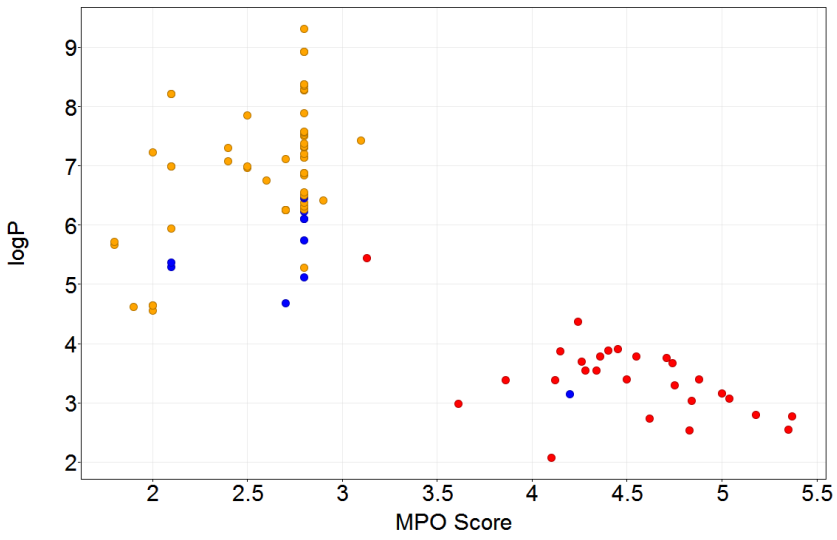

Table 1 – Biological screening data for the headgroup replacement library

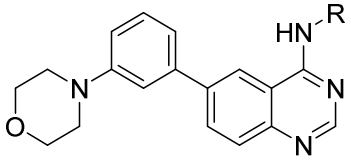

Entry	R	LogP	MPO Score	*T. brucei* EC_{50} (µM)[a]	*T. brucei* LLE
2[b] **NEU-617**	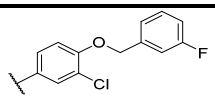	7.3	2.8	0.042	0.1
5 NEU-964	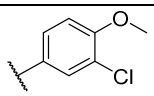	5.4	2.2	0.53	0.8
9a NEU-1939	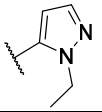	3.9	3.1	19.7	0.8
9b NEU-1940	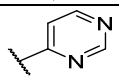	3.7	3.5	7.0	1.5
9c NEU-1942	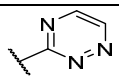	2.8	5.4	6.3	2.4
9d NEU-1943	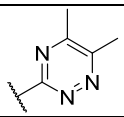	3.0	4.9	12.6	1.9
9e NEU-1944	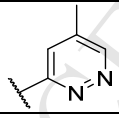	3.9	3.2	7.1	1.2
9f NEU-1945	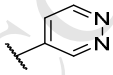	2.8	4.3	3.8	2.6
9g NEU-1946	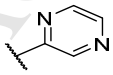	3.2	4.0	12.8	1.7
9h NEU-1959	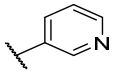	3.8	3.4	0.95	2.2

Entry	R	LogP	MPO Score	*T. brucei* EC_{50} (μM)[a]	*T. brucei* LLE
9i NEU-1960	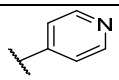	3.8	3.6	0.29	2.8
9j NEU-1961		3.8	3.9	0.32	2.7
9k NEU-1963	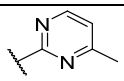	3.9	3.6	1.0	2.1
9l NEU-1964	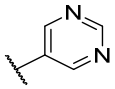	3.1	4.1	0.97	2.9
9m NEU-1965		3.4	3.8	1.4	2.5
9n NEU-1966	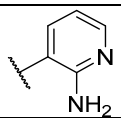	3.5	3.3	1.2	2.4
9o NEU-1967	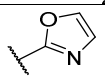	3.6	4.8	0.79	2.5
9p NEU-1968	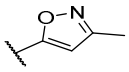	3.6	4.3	1.2	2.4
9q NEU-2071	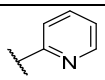	4.4	3.0	2.1	1.3
9r NEU-2072	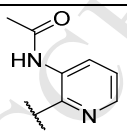	3.6	2.7	0.77	2.5
9s NEU-2073	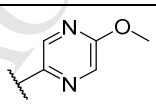	3.6	3.3	1.7	2.2
9t NEU-2075	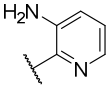	3.5	3.2	1.2	2.4

Entry	R	LogP	MPO Score	*T. brucei* EC_{50} (μM)[a]	*T. brucei* LLE
9u NEU-2079	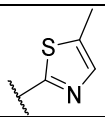	5.0	2.7	1.1	1.0
9v NEU-2080		4.3	3.4	1.4	1.5
9w NEU-2081		3.5	5.3	0.94	2.6
9x NEU-2082		3.8	3.3	0.64	2.4
10a NEU-1941	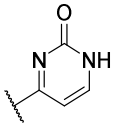	2.5	3.9	>50	nd[c]
10b NEU-2074	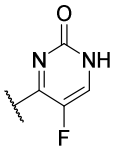	2.7	4.5	1.2	3.2

[a]Compounds showing >75% growth inhibition at 5 μM for *T.b. brucei* were tested for EC_{50} values. *T.b. brucei* EC_{50} values are the result of duplicate experiments, within ± 24%. [b]Previously reported data.[12] [c]nd=not calculated due to inactivity towards *T.b. brucei*

We also conducted an exploration on the tail region of **2** (in red, **Figure 1**). Since previous work detailed by Patel *et al.* focused primarily on potency and the SAR of the morpholine ring [12], we focused on exchanging the phenyl ring for bioisosteres to lower the LogP. Specifically, the phenyl linker in **2** was replaced with pyrimidines, triazoles, and an acyclic amide linker. We avoided the common thiophene bioisostere due to a lack of improvement in LogP when compared to **2**.

Synthesis for these new compounds expands on the previously synthesized intermediate **11** [12], shown in **Scheme 2**. The boronic ester **12** was synthesized from a Miyaura borylation reaction with the aryl iodide, followed by a Chan-Lam coupling [27, 28] to obtain the azide **13**. Both reactions proceeded in good yields. These three intermediates (**11**, **12**, **13**) were used to synthesize the 5 analogs in the phenyl replacement library. **Scheme 3** illustrates the synthetic route to the pyrimidine-linked analogs **17** and **18**, which were synthesized starting with commercially available 2,4-dichloropyrimidine **14**. Chloride displacement with morpholine afforded the two isomers **15** and **16** in a 1 to 13 ratio, which were readily separated by column chromatography. Suzuki coupling of the boronic ester **12** provided the two final isomers **17** and **18**.

The amide-linked compound **21** was synthesized from commercially available 2-chloro acetamide **19**, shown in **Scheme 4**. As previously reported [29], the acetamide underwent *in situ* halogen exchange and subsequent displacement with morpholine to afford intermediate **20**. This intermediate reacted with the aryl iodide **11** in a copper-catalyzed Buchwald amidation reaction to produce the final compound **21**.

Lastly, the triazole linkers were synthesized through methods shown in **Schemes 5** and **6**. In **Scheme 5**, the 1,2,3-triazole **23** was synthesized from a Huisgen cyclization reaction with intermediate **13** and the respective alkyne **22** adapted from Amegadzie *et al*. [30]. Use of the ruthenium catalyst selectively promotes formation of the 1,5 product whereas a copper catalyst promotes 1,4 products or a mixture of the two isomers [31]. Finally, in **Scheme 6** the commercially available dibromo-1,2,4-triazole **24** is mono-substituted with morpholine to synthesize intermediate **25**, which then undergoes a Suzuki coupling with the aryl boronic ester **12** to afford the final product **26**.

Scheme 2. Synthesis of azide intermediate **13**.

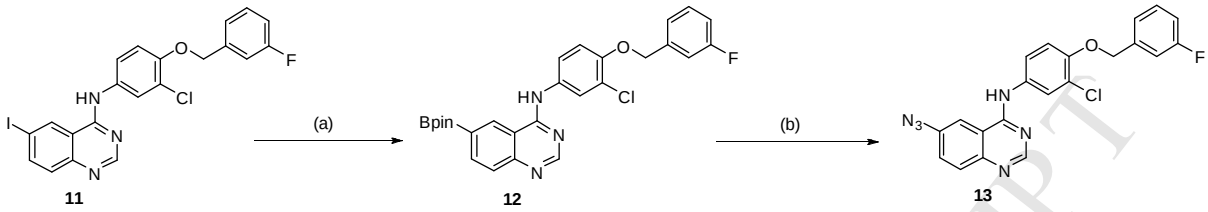

Reagents and conditions: (a) B_2pin_2, KOAc, $Pd(dppf)Cl_2$-DCM, DMF, 85°C, 12 h, 82%; (b) NaN_3, $Cu(OAc)_2$, MeOH, 55°C, 12 h, 88%.

Scheme 3. Synthesis of analogs **17** and **18**.

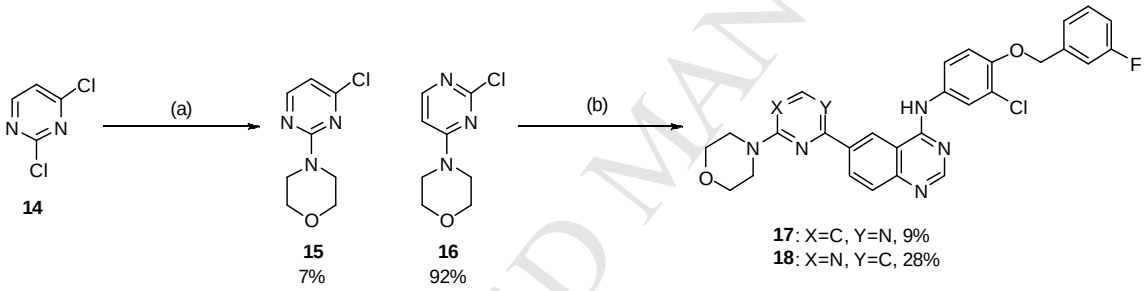

Reagents and conditions: (a) morpholine, DIPEA, *i*PrOH, 0°C to RT, 12 h; (b) 12, 2M Na_2CO_3 in H_2O, $Pd(PPh_3)_4$, DME/EtOH (3:2), 85°C, 12 h.

Scheme 4. Synthesis of **21**.

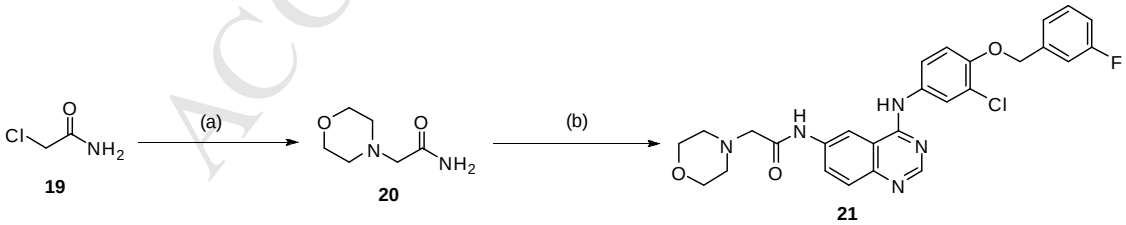

Reagents and conditions: (a) morpholine, K_2CO_3, NaI, EtOH, 85°C, 6 h, 91%; (b) **11**, Cs_2CO_3, DMEDA, CuI, THF, N_2, RT, 18 h, 37%.

Scheme 5. Preparation of analog **23**.

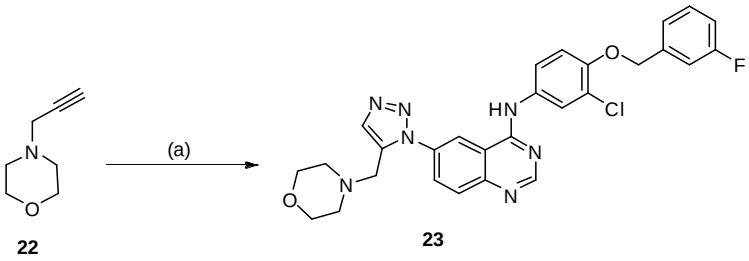

Reagents and conditions: (a) **13**, $Cp^*RuCl_2(PPh_3)_2$, 1,4-dioxane, N_2, MW, 150°C, 30 min, 13%.

Scheme 6. Preparation of compound **23.**

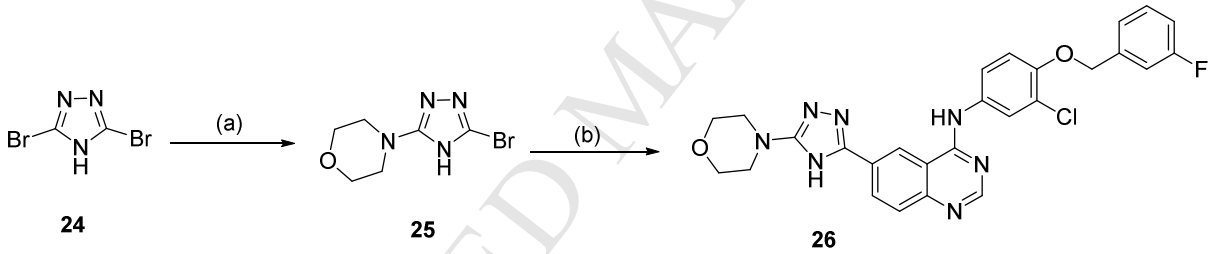

Reagents and conditions: (a) morpholine, pyridine, MW, 210°C, 10 min, 52%; (b) **12**, 2M Na_2CO_3 in H_2O, $Pd(PPh_3)_4$, DME/EtOH (3:2), 85°C, 12 h, 5%.

Biological screening data for the five phenyl replacement analogs are shown in **Table 2**. The most potent analog of the series is the pyrimidine compound **18** with an EC_{50} of 0.41 µM, a 10-fold drop in potency compared to **2**. Interestingly, the 2-morpholine substituted isomer was active while the 4-morpholine (**17**) was less-so (~3.5-fold). The amide linked analog (**21**) was 8-fold less active than **18** possibly due to lack of structural rigidity provided by the aromatic linkers. Both the 1,2,3-triazole **23** and the 1,2,4-triazole **26** had sub-micromolar potencies with EC_{50} values of 0.61 and 0.78 µM, respectively. As shown in **Figure 3**, these linker replacement

compounds (in blue) had LogP values about 1-3 units lower and relatively unchanged MPO scores when compared to **2** and its related SAR analogs (in orange). This translated to only a modest improvement in LLE (values of 0.8 and 1.1 for the amide/1,2,4-triazole and 1,2,3-triazole, respectively, compared to 0.1 for compound **2**).

Table 2 – Biological assay results of the linker replacement library.

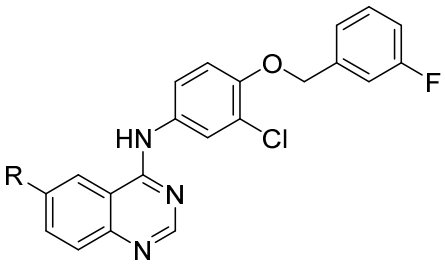

Entry	R	LogP	MPO Score	*T. brucei* EC_{50} (µM)[a]	*T. brucei* LLE
2[b]	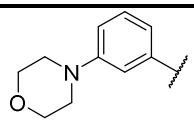	7.3	2.8	0.042	0.1
17 NEU-1008	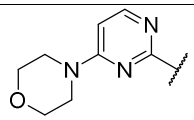	6.5	1.8	1.4	-0.6
18 NEU-1011	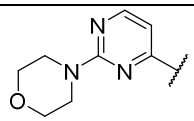	6.5	1.8	0.41	-0.1
21 NEU-1009	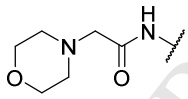	4.7	1.7	3.1	0.8
23 NEU-2083	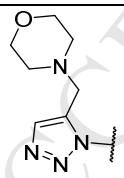	5.1	1.8	0.61	1.1
26 NEU-2078	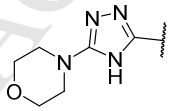	5.3	1.1	0.78	0.8

[a]Compounds showing >75% growth inhibition at 5 µM for *T.b. brucei* were tested for EC_{50} values. *T.b. brucei* EC_{50} values are the result of duplicate experiments, within ± 24%. [b]Previously reported data.[12]

With promising head and tail replacements in hand, we prepared the cross-over analogs **33a-d**, which consisted of the most potent pyrimidine linker/tail replacement of pyrimidine **18** and the 2-aminopyrimidine (**9j**) or 4-aminopyridine (**9i**) from the improved headgroup replacement library. A redesigned synthetic route was utilized (**Scheme 7**), as the sequence described for previous analogs proved to be low-yielding in these cases. Mono-bromide displacement on 2,4-dibromopyrimidine with morpholine provided isomers **28a-b** that were chromatographically separable. Preparation of the boronate ester **30** was accomplished using Miyuara borylation conditions**,** followed by a Suzuki coupling with the pyrimidine regioisomers **28a** and **28b** to provide intermediates **31a-b**. Condensation with formamide afforded the aminoquinazoline core (**32a-b**), which was arylated under Buchwald-Hartwig conditions to obtain the desired compounds **33a-d** [32, 33].

Scheme 7. Synthesis of headgroup/linker crossover analogs **33.**

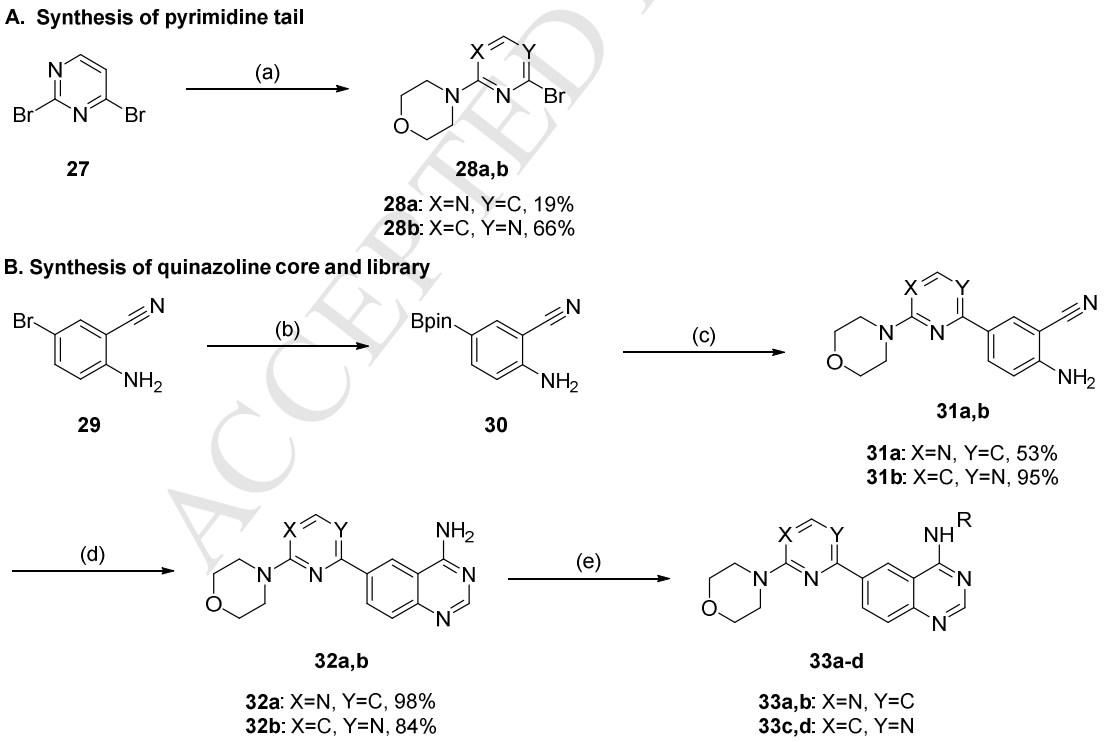

Reagents and conditions: (a) morpholine, K_2CO_3, THF, RT, 24 h; (b) B_2pin_2, KOAc, Pd(dppf)Cl2-DCM, 1,4-dioxane, MW, 130°C, 1 h, 88%; (c) **31a** or **31b**, Cs_2CO_3, $Pd(PPh_3)_4$, 1,4-dioxane/H_2O (3:1), MW, 130°C, 10 min; (d) formamide, MW, 200°C, 1 h; (e) 2-chloropyrimidine or 4-chloropyridine, $Pd_2(dba)_3$, DPPF, 1,4-dioxane, MW, 170°C, 1-2 h, 30-67%.

Screening results for the cross-over compounds **33a-d** are shown in **Table 3**. While all compounds showed at least 2-fold improved computed properties (lower LogP and higher MPO scores) over **2**, only **33d** showed activity against *T. brucei* cultures at 5.7 µM (LLE=2.2). This suggests that while we were able to observe compounds with active tail replacements (maintaining the large headgroup of **2**) and active headgroup replacements (retaining the original tail of **2**), these active compounds could potentially be mediating their effects via different targets, such that combining these structural changes abrogates some activity. Target validation efforts are underway to further explain this result.

Table 3 – Biological assay data for crossover compounds **33**.

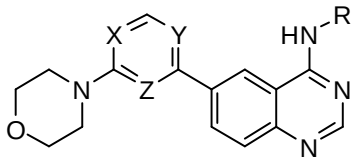

Entry	X	Y	Z	R	LogP	MPO Score	*T.brucei* EC_{50} (µM)	*T. brucei* LLE
2	C	C	C	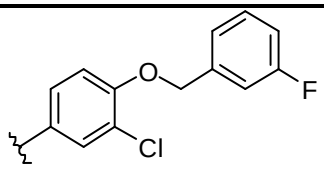	7.3	1.8	0.042	0.1
33a NEU-4436	N	C	N	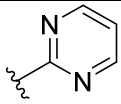	2.9	4.3	>10.0	nd[c]
33b NEU-4444	N	C	N	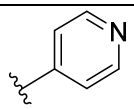	2.9	4.4	>10.0	nd[c]
33c NEU-4446	C	N	N	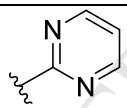	2.9	4.3	>10.0	nd[c]
33d NEU-4445	C	N	N	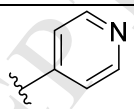	3.0	4.4	5.70	2.2

[a]Compounds showing >75% growth inhibition at 5 µM for *T.b. brucei* were tested for EC_{50} values. *T.b. brucei* EC_{50} values are the result of duplicate experiments, within ± 25%. [b]Previously reported data.[12] [c]nd=not calculated due to inactivity towards *T.b. brucei*

We have previously reported the value of screening our libraries against multiple kinetoplastid and protozoan parasites [14, 34]. Most importantly, our cross-screening campaign of lapatinib-derived analogs has produced multiple active compounds against one or more parasites in a single library [15]. We therefore tested our new analogs against the causative agents for Chagas disease (*Trypanosoma cruzi*), leishmaniasis (*Leishmania major*), and malaria (*Plasmodium falciparum*). The results are displayed in **Table 4**.

Of the 35 new compounds, the oxazole analog **9o** was the only analog found to be active against *T. cruzi* and *L. major* amastigotes with EC_{50} values of 0.060, and 0.67 µM, respectively; further studies of this compound against these pathogens are underway and will be reported in due course. Interestingly, other researchers have also denoted the ability of oxazole compounds to show activity against related kinetoplastids *T. brucei*, *T. cruzi*, and leishmaniasis [35]. Nearly all of the linker replacements showed activity towards *P. falciparum* D6 with the pyrimidines **17** and **18** (EC_{50} = 0.93 and 0.069 µM, respectively), amide **21** (0.53 µM), and 1,2,4-triazole **26** (0.21 µM) being the most potent analogs from all the compounds screened against *P. falciparum* D6. As seen with *T. brucei*, the 2-morpholine substituted pyrimidine **18** was 13.5-fold more active than its isomer **17** against *P. falciparum.* The cross-over analog **33b** with pyrimidines in both the linker (same stereochemistry as **18**) and headgroup replacements had an EC_{50} of 0.31 µM against *P. falciparum* D6. Only **9c** showed meaningful toxicity to the HepG2 cell line with a TC_{50} of 4 µM. Additional screening data, such as that for *L. major* promastigotes and *P. falciparum* strains W2 and C235, can be found in the Supporting Information (**Tables S.2 and S.3**)

Table 4 – Cross-screening data for all compounds.

Entry	*T.b. brucei* EC_{50} (µM)[a]	*T. cruzi* EC_{50} (µM)[a]	*L. major* Amastigotes EC_{50} (µM)[b]	*P. falciparum* D6 EC_{50} (µM)[c]	NIH 3T3 TC_{50} (µM)	HepG2 TC_{50} (µM)
2[d]	0.042	1.8	7.98	0.23	>50	>30
5	0.53	>50	>15	1.87	>100	>30
9a	19.7	>50	>15	2.87	>100	>30
9b	7.0	10.6	>15	3.21	>50	>30
9c	6.3	8.9	>15	>15	39	4.0
9d	12.6	27.2	>15	2.60	>50	>20
9e	7.1	13.9	>15	5.59	>50	>30
9f	3.8	>50	8.78	1.01	>100	>30
9g	12.8	>50	>15	6.62	>100	>30
9h	0.95	31.5	>15	>15	38	>30
9i	0.29	3.4	>15	>15	>100	>30
9j	0.32	32.2	>15	>15	>100	>30
9k	1.0	23.9	>15	>15	>100	>30
9l	0.97	22.5	>15	14.17	22	>30

Entry	*T.b. brucei* EC_{50} (μM)[a]	*T. cruzi* EC_{50} (μM)[a]	*L. major* Amastigotes EC_{50} (μM)[b]	*P. falciparum* D6 EC_{50} (μM)[c]	NIH 3T3 TC_{50} (μM)	HepG2 TC_{50} (μM)
9m	1.4	27.0	>15	10.56	>50	>30
9n	1.2	6.5	>15	5.71	>50	>30
9o	0.79	0.06	0.67	5.16	>100	22
9p	1.2	2.7	12.50	13.45	12	>30
9q	2.1	>20	5.22	5.22	nd[d]	>30
9r	0.77	>50	22.70	22.70	nd[d]	>30
9s	1.7	11.0	24.13	>15	nd[d]	>20
9t	1.2	13.9	25.09	8.16	nd[d]	>30
9u	1.1	5.1	4.96	4.17	13	13.4
9v	1.4	2.2	6.60	>15	8.1	14.6
9w	0.94	14.7	25.61	>15	nd[d]	>30
9x	0.64	>50	25.68	7.56	nd[d]	>30
10a	>50	>50	>15	>15	>100	>30
10b	1.2	>20	23.90	>20	nd[d]	>30
17	1.4	4.8	>3	0.93	36	>20
18	0.41	24.4	>15	0.069	47	>20

Entry	*T.b. brucei* EC_{50} (μM)[a]	*T. cruzi* EC_{50} (μM)[a]	*L. major* Amastigotes EC_{50} (μM)[b]	*P. falciparum* D6 EC_{50} (μM)[c]	NIH 3T3 TC_{50} (μM)	HepG2 TC_{50} (μM)
21	3.1	6.9	8.11	0.53	9.1	>20
23	0.61	>15	6.34	6.05	>50	>20
26	0.78	7.6	1.88	0.21	>50	>20
33a	>10.0	15	25.88	25.88	>50	>30
33b	>10.0	>50	25.95	0.31	>50	>30
33c	>10.0	>50	25.88	11.12	>50	14.8
33d	5.7	0.37	25.95	1.04	>50	>30

[a]Compounds showing >75% growth inhibition at 5 or 10 μM for *T.b. brucei* or *T. cruzi* respectively, were tested for EC_{50} values. *T.b. brucei* EC_{50} values are the result of duplicate experiments, within ± 24%. *T. cruzi* EC_{50} values are the result of duplicate experiments, within ± 24%, with the exception of **2** (± 50%) and **6p** (± 100%). [b]Compounds screened against *L. major* amastigotes had r^2 values >0.75. [c]Compounds tested in duplicate against *P. falciparum* (D6 strain) had r^2 values >0.80. [d]Previously reported data.[12, 15]

Lastly, most compounds were also screened for their ADME properties (Supporting Information **Table S.4**). A few representative compounds are shown below in **Table 5**. While majority of the compounds that were screened had human plasma protein binding of 90-99%, only **33a** and **33c** had values below 90%. All but 6 of the screened compounds had desired human microsome clearance of <90 µL/min/mg, whereas only 10 out of the 27 compounds had the desired rat hepatocytes clearance of <55 µL/min/10^6 cells. Despite almost all analogs having a slightly improved aqueous solubility over **2**, only **9a** and **33c** were significantly improved and over the targeted value of 100 µM (288 and >1000 µM respectively). Even though all compounds had reduced lipophilicity (LogP) values by design, this did not translate into increased aqueous solubility across all of the analogs. Therefore, it can be concluded that aqueous solubility is not dependent on LogP and these two factors do not correlate in this chemical series.

Table 5 – ADME properties for selective compounds.

Entry	LogP	Aqueous Solubility (µM)	Human Plasma Protein Binding %	Human Microsome Cl_{int} (µL/min/mg)	Rat Hepatocytes Cl_{int} (µL/min/10^6 cells)
2 NEU-617	7.31	<1	99	63.0	44.5
9a NEU-1939	3.87	288.0	93.9	60.9	99.5
9i NEU-1960	3.78	2.9	98.8	80.2	47.2
9j NEU-1961	3.75	16.7	93.8	33.3	25.4

Entry	LogP	Aqueous Solubility (µM)	Human Plasma Protein Binding %	Human Microsome Cl_{int} (µL/min/mg)	Rat Hepatocytes Cl_{int} (µL/min/10^6 cells)
9o NEU-1967	3.62	2.3	99.0	50.9	46.9
18 NEU-1011	6.45	<1	99.8	nd[a]	nd[a]
33a NEU-4436	2.89	29.0	88	71.3	20.3
33c NEU-4446	2.89	>1000	86	10.1	26.5

[a]Not determined (nd)

3. Conclusions

We initially set out to improve the physicochemical properties of **2** by designing compounds with improved LogP and MPO scores in order to achieve a better drug candidate with higher LLE values. We specifically targeted the headgroup region of the molecule by exploring truncated or small aminoheterocycles generated by *in silico* design, as well as replacement of the tail region with other polar moieties. From these libraries, we discovered 12 compounds with sub-micromolar EC_{50} values against *T. brucei*, all of which had significantly improved LogP and MPO scores over **2**, and almost all had improved LLE values. Of those compounds, the pyridine **9i** (EC_{50} = 0.29 µM) and pyrimidines **9j** (0.32 µM) and **18** (0.41 µM) were utilized in the design of cross-over compounds, matching the best and most potent components of each library, though despite their improved LogP and MPO scores, there was a

significant reduction in potency. Throughout this series, aqueous solubility remains a significant challenge to be surmounted, noting that the poor solubility does not correlate with LogP.

In addition to screening against *T. brucei*, all compounds were screened against related protozoan parasites *T. cruzi*, *L. major*, and *P. falciparum*. Interestingly, analog **9o** not only showed sub-micromolar potency towards *T. brucei* (EC_{50} = 0.79 µM), but it was potent against both *T. cruzi* and *L. major* amastigotes (EC_{50} = 0.06 and 0.67 µM, respectively). Plus 4 out 5 compounds (**17**, **18**, **21**, **26**) in the tail optimization library and cross-over compound **33b** displayed sub-micromolar activity towards *P. falciparum* D6. We continue optimization efforts in this chemical series against these four protozoan pathogens, with an eye towards improved pharmacokinetics and in vivo efficacy.

4. Materials and Methods

4.1 Chemical synthesis.

Unless otherwise noted, reagents were obtained from Sigma-Aldrich, Inc. (St. Louis, MO) or Fisher Scientific, and used as received. NMR spectra were obtained on a Varian NMR system, operating at 400 MHz and 500 MHz for 1H acquisitions. Spectrum were analyzed using ACD/Labs NMR processing software. GCMS analysis was performed using an Agilent HP 6890 gas chromatograph with an Agilent HP5973 transmission quadrupole mass spectrometer (electron impact). LCMS analysis was performed using a Waters e2795 Alliance reverse-phase HPLC-MS and 3.5 µm Waters SunFire C18 4.6x50mm or Waters SunFire 3.5 µm C8 4.6x50mm columns, with single-wavelength Waters 2489 UV-visible detector (λ = 254 nm) or multiwavelength Waters 2996 photodiode array detector (λ = 200-600 nm) and Waters LCTPremier time-of-flight mass spectrometer (electrospray ionization) or MicroMass ZQ single

quadropole mass spectrometer (electrospray ionization). Preparative HPLC was performed using a Waters FractionLynx and 5 µm Waters Symmetry C8 30x50mm or 5 µm Waters Xbridge OBD RP18 30x50mm columns, with single-wavelength Waters 2489 UV-visible detector (λ = 254 nm) and MicroMass ZQ mass spectrometer (electrospray ionization). Gradients for the LCMS analysis and preparative HPLC were water or acetonitrile, both with 0.1% v/v formic acid. Purest fractions from the preparative HPLC and Biotage Isolera One reverse phase chromatography with Biotage SNAP C18 columns provided the percent yields reported and any impure fractions were discarded. All newly synthesized compounds were deemed >95% pure by LCMS and NMR analysis.

6-(3-morpholinophenyl)quinazolin-4(3H)-one (7). 6-iodoquinazolin-4(3H)-one (0.672 g, 2.469 mmol), 4-(3-(4,4,5,5-tetramethyl-1,3,2-dioxaborolan-2-yl)phenyl)morpholine (1.785 g, 6.17 mmol), a 2 M aqueous solution of sodium carbonate (7.41 mL, 14.81 mmol), [1,1'-bis(diphenylphoshpino)ferrocene] dichloropalladium(II) dichloromethane adduct (0.141 g, 0.173 mmol), dimethoxyethane (5 mL), and ethanol (3.3 mL) were added together and heated at 85^{o}C for 6 h. The reaction mixture was concentrated under reduced pressure, filtered through celite, and the product was collected by silica column chromatography (dichloromethane/methanol). The collected fractions were concentrated under reduced pressure. A mixture of 70% hexanes/30% toluene was added and the precipitated product was collected by vacuum filtration to obtain a 66% yield as a tan solid. ^{1}H NMR (500 MHz, DMSO-d_6) δ ppm 3.21 (m, 4 H), 3.76 (m, 4 H), 7.00 (dd, J = 8.3, 2.4 Hz, 1 H), 7.17 (d, J = 7.8 Hz, 1 H), 7.25 (m, 1 H), 7.36 (t, J = 7.8 Hz, 1 H), 7.74 (d, J = 8.3 Hz, 1 H), 8.12 (m, 2 H), 8.31 (d, J = 2.0 Hz, 1 H), 12.31 (br. s, 1 H). LCMS found 308.1, $[M+H]^{+}$.

4-(3-(4-chloroquinazolin-6-yl)phenyl)morpholine (8). A flask with septum containing both **7** (0.350 g, 1.137 mmol) and triphenylphosphine (0.597 g, 2.274 mmol) was purged with nitrogen three times. Anhydrous 1,2-dichloroethane (12 mL) was added and allowed to stir for 5 mins, followed by the addition of carbon tetrachloride dropwise (0.329 mL, 3.410 mmol). The reaction was stirred at 70^{o}C for 12 h. The reaction mixture was concentrated under reduced pressure and purified by silica column chromatography (hexanes/ethyl acetate) to obtain the product in 97% yield as a yellow solid. ^{1}H NMR (500 MHz, DMSO-d_6) δ ppm 3.25 (m, 4 H), 3.79 (m, 4 H), 7.09 (d, J = 7.3 Hz, 1 H), 7.24 (d, J = 7.3 Hz, 1 H), 7.34 (s, 1 H), 7.39 (t, J = 7.8 Hz, 1 H), 7.79 (d, J = 8.3 Hz, 1 H), 8.18 (dd, J = 8.5, 2.2 Hz, 1 H), 8.34 (d, J = 2.0 Hz, 1 H), 8.39 (s, 1 H). LCMS found 326.1, $[M+H]^{+}$.

N-(2-aminopyridin-3-yl)acetamide [36]. To a solution of pyridine-2,3-diamine (0.207 g, 1.896 mmol) and pyridine (0.307 mL, 3.79 mmol) in anhydrous THF (7 mL) cooled at 0^{o}C was added acetic anhydride (0.197 mL, 2.086 mmol) dropwise. The reaction mixture stirred at 0^{o}C for 30 mins and then at room temperature for 12 h. The product was purified by silica column chromatography (ethyl acetate/methanol) to obtain the product in 61% yield as a light brown solid. ^{1}H NMR (500 MHz, DMSO-d_6) δ ppm 2.05 (s, 3 H), 5.75 (s, 2 H), 6.54 (dd, J = 7.8, 4.9 Hz, 1 H), 7.59 (dd, J = 7.3, 1.5 Hz, 1 H), 7.76 (dd, J = 4.6, 1.7 Hz, 1 H), 9.11 (s, 1 H). LCMS found 151.7, $[M+H]^{+}$.

Reaction Conditions for Buchwald Library. To a flame-dried flask was added **8** (0.046 g, 0.142 mmol), xantphos (0.016 g, 0.028 mmol), potassium carbonate (0.392 g, 2.83 mmol), palladium(II) acetate (0.003 g, 0.014 mmol), and the respective amine (0.170 mmol). The flask was purged with nitrogen three times and then anhydrous dioxane (1.5 mL) was added under nitrogen. The reaction was refluxed at 105^{o}C for 12 h while under nitrogen, maintaining a

positive pressure. The mixture was concentrated under reduced pressure, separated by silica column chromatography (dichloromethane/isopropanol), and purified by reverse phase chromatography (water/acetonitrile).

N-(3-chloro-4-methoxyphenyl)-6-(3-morpholinophenyl)quinazolin-4-amine (5). (Pale yellow solid, Yield: 28%). ^{1}H NMR (500 MHz, DMSO-d_6) δ ppm 3.24 (m, 4 H), 3.79 (m, 4 H), 3.88 (s, 3 H), 7.03 (dd, *J* = 8.3, 2.0 Hz, 1 H), 7.22 (d, *J* = 9.3 Hz, 1 H), 7.31 (d, *J* = 7.8 Hz, 1 H), 7.35 (t, *J* = 2.0 Hz, 1 H), 7.41 (t, *J* = 7.8 Hz, 1 H), 7.75 (dd, *J* = 9.3, 2.9 Hz, 1 H), 7.84 (d, *J* = 8.3 Hz, 1 H), 8.00 (d, *J* = 2.4 Hz, 1 H), 8.18 (dd, *J* = 8.8, 2.0 Hz, 1 H), 8.58 (s, 1 H), 8.76 (d, *J* = 2.0 Hz, 1 H), 9.88 (s, 1 H). LCMS found 447.1, $[M+H]^+$.

N-(1-ethyl-1H-pyrazol-5-yl)-6-(3-morpholinophenyl)quinazolin-4-amine (9a). (Yellow solid, Yield: 27%). ^{1}H NMR (400 MHz, DMSO-d_6) δ ppm 1.31 (t, J = 7.0 Hz, 3 H), 3.23 (m, 4 H), 3.79 (m, 4 H), 3.97 (m, 2 H), 6.26 (s, 1 H), 7.02 (dd, *J* = 8.4, 1.8 Hz, 1 H), 7.37 (m, 3 H), 7.51 (s, 1 H), 7.86 (m, 1 H), 8.22 (m, 1 H), 8.51 (m, 1 H), 8.72 (s, 1 H), 9.98 (s, 1 H). LCMS found 401.2, $[M+H]^+$.

6-(3-morpholinophenyl)-N-(pyrimidin-4-yl)quinazolin-4-amine (9b). (Yellow solid, Yield: 59%). ^{1}H NMR (500 MHz, DMSO-d_6) δ ppm 3.24 (m, 4 H), 3.80 (m, 4 H), 7.03 (m, 1 H), 7.41 (m, 3 H), 7.95 (d, *J* = 8.8 Hz, 1 H), 8.29 (dd, *J* = 8.8, 2.0 Hz, 1 H), 8.55 (s, 1 H), 8.72 (d, *J* = 5.9 Hz, 1 H), 8.85 (s, 1 H), 8.98 (m, 2 H), 11.05 (m, 1 H). LCMS found 385.2, $[M+H]^+$.

6-(3-morpholinophenyl)-N-(1,2,4-triazin-3-yl)quinazolin-4-amine (9c). (Yellow solid, Yield: 55%). ^{1}H NMR (400 MHz, DMSO-d_6) δ ppm 3.21 (m, 4 H), 3.77 (m, 4 H), 7.02 (dd, *J* = 8.4, 1.8 Hz, 1 H), 7.29 (d, *J* = 7.3 Hz, 1 H), 7.38 (m, 2 H), 7.89 (d, *J* = 8.8 Hz, 1 H), 8.25 (dd, *J* = 8.8, 1.5 Hz, 1 H), 8.63 (s, 1 H), 8.76 (d, *J* = 2.2 Hz, 1 H), 8.78 (d, *J* = 2.2 Hz, 1 H), 9.13 (d, *J* = 2.2 Hz, 1 H), 12.04 (s, 1 H). LCMS found 386.2, $[M+H]^+$.

6-(3-morpholinophenyl)-N-(1,2,4-triazin-3-yl)quinazolin-4-amine (9d). (Yellow solid, Yield: 5%). ^{1}H NMR (400 MHz, DMSO-d_6) δ ppm 2.53 (s, 2 H), 2.61 (s, 3 H), 3.23 (m, 4 H), 3.78 (m, 4 H), 7.02 (dd, *J* = 8.4, 1.8 Hz, 1 H), 7.39 (m, 3 H), 7.86 (m, 1 H), 8.24 (d, *J* = 7.3 Hz, 1 H), 8.57 (s, 1 H), 8.75 (s, 1 H), 11.29 (s, 1 H). LCMS found 414.2, $[M+H]^+$.

N-(5-methylpyridazin-3-yl)-6-(3-morpholinophenyl)quinazolin-4-amine (9e). (Yellow solid, Yield: 7%). ^{1}H NMR (400 MHz, DMSO-*d6*) δ ppm 2.40 (s, 3 H), 3.25 (m, 5 H), 3.80 (m, 5 H), 7.03 (m, 1 H), 7.41 (m, 3 H), 7.91 (d, *J* = 8.8 Hz, 1 H), 8.27 (d, *J* = 8.1 Hz, 1 H), 8.47 (s, 1 H), 8.70 (s, 1 H), 8.90 (s, 1 H), 9.02 (s, 1 H), 11.13 (s, 1 H). LCMS found 399.2, $[M+H]^+$.

6-(3-morpholinophenyl)-N-(pyridazin-4-yl)quinazolin-4-amine (9f). (Pale red solid, Yield: 59%). ^{1}H NMR (400 MHz, DMSO-d_6) δ ppm 3.24 (m, 4 H), 3.79 (m, 4 H), 7.06 (dd, *J* = 8.1, 2.2 Hz, 1 H), 7.31 (d, *J* = 7.3 Hz, 1 H), 7.37 (s, 1 H), 7.43 (t, *J* = 8.1 Hz, 1 H), 7.96 (d, *J* = 8.8 Hz, 1 H), 8.27 (dd, *J* = 8.8, 1.5 Hz, 1 H), 8.40 (m, 1 H), 8.83 (s, 2 H), 9.11 (d, *J* = 5.9 Hz, 1 H), 9.74 (s, 1 H), 10.33 (s, 1 H). LCMS found 385.2, $[M+H]^+$.

6-(3-morpholinophenyl)-N-(pyrazin-2-yl)quinazolin-4-amine (9g). (Yellow solid, Yield: 49%). ^{1}H NMR (400 MHz, DMSO-d_6) δ ppm 3.24 (m, 4 H), 3.79 (m, 4 H), 7.02 (m, 1 H), 7.40 (m, 3 H), 7.91 (d, *J* = 8.8 Hz, 1 H), 8.27 (d, *J* = 8.8 Hz, 1 H), 8.40 (d, *J* = 1.5 Hz, 1 H), 8.51 (s, 1 H), 8.74 (s, 1 H), 8.99 (s, 1 H), 9.66 (s, 1 H), 10.87 (s, 1 H). LCMS found 385.2, $[M+H]^+$.

6-(3-morpholinophenyl)-N-(pyridin-3-yl)quinazolin-4-amine (9h). (Yellow solid, Yield: 49%). ^{1}H NMR (500 MHz, DMSO-d_6) δ ppm 3.24 (m, 4 H), 3.79 (m, 4 H), 7.03 (dd, *J* = 8.1, 2.2 Hz, 1 H), 7.31 (d, *J* = 7.8 Hz, 1 H), 7.36 (m, 1 H), 7.41 (t, *J* = 7.8 Hz, 1 H), 7.46 (dd, *J* = 8.3, 4.9 Hz, 1 H), 7.87 (d, *J* = 8.8 Hz, 1 H), 8.21 (dd, *J* = 8.8, 2.0 Hz, 1 H), 8.31 (ddd, *J* = 8.3, 2.4, 1.5 Hz, 1 H), 8.35 (dd, *J* = 4.9, 1.5 Hz, 1 H), 8.62 (s, 1 H), 8.80 (d, *J* = 2.0 Hz, 1 H), 9.02 (d, *J* = 2.4 Hz, 1 H), 10.06 (s, 1 H). LCMS found 384.1, $[M+H]^+$.

6-(3-morpholinophenyl)-N-(pyridin-4-yl)quinazolin-4-amine (9i). (Yellow solid, Yield: 26%). ^{1}H NMR (500 MHz, DMSO-d_6) δ ppm 3.24 (m, 4 H), 3.79 (m, 4 H), 7.04 (dd, *J* = 8.3, 2.0 Hz, 1 H), 7.31 (d, *J* = 7.8 Hz, 1 H), 7.36 (m, 1 H), 7.42 (t, *J* = 7.8 Hz, 1 H), 7.92 (d, *J* = 8.8 Hz, 1 H), 8.03 (m, 2 H), 8.24 (dd, *J* = 8.8, 2.0 Hz, 1 H), 8.52 (m, 2 H), 8.77 (s, 1 H), 8.83 (d, *J* = 2.0 Hz, 1 H), 10.12 (s, 1 H). LCMS found 384.2, $[M+H]^+$.

6-(3-morpholinophenyl)-N-(pyrimidin-2-yl)quinazolin-4-amine (9j). (Pale yellow solid, Yield: 21%). ^{1}H NMR (400 MHz, 1:1 $CD_3OD/CDCl_3$) δ ppm 3.28 (m, 4 H), 3.92 (m, 4 H), 7.01 (d, *J* = 7.3 Hz, 1 H), 7.14 (m, 1 H), 7.29 (d, *J* = 7.3 Hz, 1 H), 7.40 (m, 2 H), 7.76 (m, 1 H), 8.11 (m, 2 H), 8.79 (m, 3 H). LCMS found 385.1, $[M+H]^+$.

N-(4-methylpyrimidin-2-yl)-6-(3-morpholinophenyl)quinazolin-4-amine (9k). (Yellow solid, Yield: 10%). ^{1}H NMR (400 MHz, DMSO-d_6) δ ppm 2.47 (s, 3 H), 3.23 (m, 5 H), 3.78 (m, 5 H), 7.02 (dd, *J* = 8.8, 2.2 Hz, 1 H), 7.10 (m, 1 H), 7.39 (m, 3 H), 7.87 (m, 1 H), 8.22 (m, 1 H), 8.58 (d, *J* = 5.1 Hz, 1 H), 8.72 (m, 2 H), 10.83 (s, 1 H). LCMS found 399.2, $[M+H]^+$.

6-(3-morpholinophenyl)-N-(pyrimidin-5-yl)quinazolin-4-amine (9l). (Pale yellow solid, Yield: 78%). ^{1}H NMR (400 MHz, DMSO-d_6) δ ppm 3.23 (m, 4 H), 3.78 (m, 4 H), 7.04 (dd, *J* = 8.1, 1.5 Hz, 1 H), 7.30 (d, *J* = 7.3 Hz, 1 H), 7.35 (s, 1 H), 7.42 (t, *J* = 8.1 Hz, 1 H), 7.89 (d, *J* = 8.8 Hz, 1 H), 8.22 (dd, *J* = 8.8, 1.5 Hz, 1 H), 8.67 (s, 1 H), 8.77 (d, *J* = 1.5 Hz, 1 H), 8.95 (s, 1 H), 9.31 (s, 2 H), 10.18 (s, 1 H). LCMS found 385.1, $[M+H]^+$.

6-(3-morpholinophenyl)-N-(pyridazin-3-yl)quinazolin-4-amine (9m). (Yellow solid, Yield: 35%). ^{1}H NMR (400 MHz, DMSO-d_6) δ ppm 3.24 (m, 4 H), 3.79 (m, 4 H), 7.03 (m, 1 H), 7.41 (m, 3 H), 7.75 (dd, *J* = 9.2, 4.8 Hz, 1 H), 7.91 (d, *J* = 8.1 Hz, 1 H), 8.28 (d, *J* = 8.8 Hz, 1 H), 8.59 (s, 1 H), 8.70 (s, 1 H), 9.01 (m, 2 H), 11.24 (s, 1 H). LCMS found 385.1, $[M+H]^+$.

N3-(6-(3-morpholinophenyl)quinazolin-4-yl)pyridine-2,3-diamine (9n). (Yellow solid, Yield: 16%). ^{1}H NMR (500 MHz, DMSO-d_6) δ ppm 3.23 (m, 4 H), 3.78 (m, 4 H), 5.10 (s, 1 H), 5.63 (s, 1 H), 6.86 (m, 0.5 H), 7.01 (m, 1.5 H), 7.11 (m, 0.5 H), 7.17 (m, 0.5 H), 7.28 (m, 1 H), 7.37 (m, 2 H), 7.63 (m, 1 H), 7.75 (d, *J* = 3.4 Hz, 0.5 H), 7.83 (d, *J* = 8.8 Hz, 0.5 H), 7.99 (dd, *J* = 8.3, 1.5 Hz, 0.5 H), 8.19 (d, *J* = 8.8 Hz, 0.5 H), 8.26 (s, 0.5 H), 8.44 (s, 0.5 H), 8.79 (m, 1 H), 10.08 (s, 1 H). ^{1}H NMR (400 MHz, $CDCl_3$) δ ppm 3.27 (m, 4 H), 3.91 (m, 4 H), 4.62 (s, 2 H), 6.84 (dd, *J* = 7.3, 5.1 Hz, 1 H), 6.98 (m, 1 H), 7.04 (d, *J* = 7.3 Hz, 1 H), 7.21 (m, 2 H), 7.41 (t, *J* = 8.1 Hz, 1 H), 7.72 (d, *J* = 8.1 Hz, 2 H), 7.89 (dd, *J* = 8.1, 2.2 Hz, 1 H), 8.14 (s, 1 H), 8.68 (d, *J* = 2.2 Hz, 1 H). LCMS found 399.1, $[M+H]^+$.

N-(6-(3-morpholinophenyl)quinazolin-4-yl)oxazol-2-amine (9o). (Yellow solid, Yield: 24%). ^{1}H NMR (500 MHz, DMSO-d_6) δ ppm 3.22 (m, 4 H), 3.77 (m, 4 H), 7.03 (dd, *J* = 8.3, 2.0 Hz, 1 H), 7.18 (m, 1 H), 7.25 (t, *J* = 2.0 Hz, 1 H), 7.32 (d, *J* = 1.0 Hz, 1 H), 7.38 (t, *J* = 7.8 Hz, 1 H), 7.76 (d, *J* = 8.3 Hz, 1 H), 7.88 (d, *J* = 1.0 Hz, 1 H), 8.14 (dd, *J* = 8.6, 2.2 Hz, 1 H), 8.41 (s, 1 H), 8.56 (d, *J* = 2.4 Hz, 1 H), 13.35 (s, 1 H). LCMS found 374.1, $[M+H]^+$.

3-methyl-N-(6-(3-morpholinophenyl)quinazolin-4-yl)isoxazol-5-amine (9p). (Yellow solid, Yield: 49%). ^{1}H NMR (500 MHz, DMSO-d_6) δ ppm 2.26 (s, 3 H), 3.24 (m, 4 H), 3.79 (m, 4 H), 6.60 (s, 1 H), 7.03 (dd, *J* = 8.1, 2.2 Hz, 1 H), 7.34 (m, 2 H), 7.40 (t, *J* = 7.8 Hz, 1 H), 7.86 (s, 1 H), 8.24 (m, 1 H), 8.71 (s, 1 H), 8.87 (s, 1 H), 11.72 (s, 1 H). LCMS found 388.1, $[M+H]^+$.

6-(3-morpholinophenyl)-N-(pyridin-2-yl)quinazolin-4-amine (9q). (Pale yellow solid, Yield: 26%). ^{1}H NMR (500 MHz, 1:1 $CDCl_3$/CD_3OD) δ ppm 3.31 (m, 4 H), 3.93 (m, 4 H), 7.03 (dd, *J* = 8.3, 2.4 Hz, 1 H), 7.15 (t, *J* = 5.9 Hz, 1 H), 7.30 (d, *J* = 7.3 Hz, 1 H), 7.35 (m, 1 H), 7.44 (t, *J* = 7.8 Hz, 1 H), 7.88 (t, *J* = 7.3 Hz, 1 H), 7.95 (d, *J* = 8.3 Hz, 1 H), 8.15 (d, *J* = 8.3 Hz, 1 H), 8.37 (m, 1 H), 8.51 (s, 1 H), 8.70 (m, 1 H), 8.76 (s, 1 H). LCMS found 384.1, $[M+H]^+$.

N-(2-((6-(3-morpholinophenyl)quinazolin-4-yl)amino)pyridin-3-yl)acetamide (9r). (Yellow solid, Yield: 55%). ^{1}H NMR (500 MHz, 1:1 $CDCl_3$/CD_3OD) δ ppm 2.27 (s, 3 H), 3.27 (m, 4 H), 3.91 (m, 4 H), 7.03 (dd, *J* = 8.3, 2.4 Hz, 2 H), 7.24 (d, *J* = 7.3 Hz, 1 H), 7.28 (s, 1 H), 7.42 (t, *J* = 7.8 Hz, 1 H), 7.69 (d, *J* = 8.3 Hz, 1 H), 7.99 (d, *J* = 8.8 Hz, 1 H), 8.06 (d, *J* = 3.9 Hz, 1 H), 8.18 (s, 1 H), 8.64 (s, 1 H), 8.67 (d, *J* = 7.8 Hz, 1 H). LCMS found 441.1, $[M+H]^+$.

N-(5-methoxypyrazin-2-yl)-6-(3-morpholinophenyl)quinazolin-4-amine (9s). (Yellow solid, Yield: 38%). ^{1}H NMR (500 MHz, 1:1 $CDCl_3$/CD_3OD) δ ppm 3.29 (m, 4 H), 3.92 (m, 4 H), 4.01 (s, 3 H), 7.02 (dd, *J* = 8.3, 2.4 Hz, 1 H), 7.30 (d, *J* = 7.8 Hz, 1 H), 7.37 (m, 1 H), 7.43 (t, *J* = 7.8 Hz, 1 H), 7.91 (d, *J* = 8.8 Hz, 1 H), 8.08 (d, *J* = 1.5 Hz, 1 H), 8.14 (dd, *J* = 8.6, 1.7 Hz, 1 H), 8.57 (d, *J* = 2.0 Hz, 1 H), 8.68 (s, 1 H), 9.25 (m, 1 H). LCMS found 415.1, $[M+H]^+$.

5-methyl-N-(6-(3-morpholinophenyl)quinazolin-4-yl)thiazol-2-amine (9u). (Pale red solid, Yield: 20%). ^{1}H NMR (500 MHz, 1:1 $CDCl_3$/CD_3OD) δ ppm 2.45 (m, 3 H), 3.30 (m, 4 H), 3.93 (m, 4 H), 7.02 (dd, *J* = 8.3, 2.4 Hz, 1 H), 7.15 (d, *J* = 1.5 Hz, 1 H), 7.29 (m, 1 H), 7.34 (t, *J* = 2.0 Hz, 1 H), 7.42 (t, *J* = 7.8 Hz, 1 H), 7.88 (d, *J* = 8.8 Hz, 1 H), 8.12 (dd, *J* = 8.8, 2.0 Hz, 1 H), 8.64 (d, *J* = 2.0 Hz, 1 H), 8.67 (s, 1 H). LCMS found 404.1, $[M+H]^+$.

N-(6-(3-morpholinophenyl)quinazolin-4-yl)thiazol-2-amine (9v). (Yellow solid, Yield: 9%). ^{1}H NMR (500 MHz, 1:1 $CDCl_3$/CD_3OD) δ ppm 3.31 (m, 4 H), 3.93 (m, 4 H), 7.03 (dd, *J* = 8.1, 2.2 Hz, 1 H), 7.13 (d, *J* = 3.9 Hz, 1 H), 7.30 (m, 1 H), 7.36 (m, 1 H), 7.43 (t, *J* = 8.1 Hz, 1 H), 7.54 (d, *J* = 3.9 Hz, 1 H), 7.91 (m, 1 H), 8.15 (dd, *J* = 8.3, 1.5 Hz, 1 H), 8.68 (d, *J* = 2.0 Hz, 1 H), 8.74 (s, 1 H). LCMS found 390.1, $[M+H]^+$.

N-(6-(3-morpholinophenyl)quinazolin-4-yl)-1,3,4-thiadiazol-2-amine (9w). (Yellow solid, Yield: 4%). ^{1}H NMR (500 MHz, $CDCl_3$) δ ppm 3.28 (m, 4 H), 3.91 (m, 4 H), 7.00 (m, 1 H), 7.23

(m, 2 H), 7.41 (m, 1 H), 7.83 (d, *J* = 8.8 Hz, 1 H), 8.03 (d, *J* = 8.3 Hz, 1 H), 8.21 (s, 1 H), 8.74 (s, 1 H), 8.83 (s 1 H). LCMS found 391.1, $[M+H]^+$.

N-(6-(3-morpholinophenyl)quinazolin-4-yl)thiazol-5-amine (9x). (Yellow solid, Yield: 9%). ^{1}H NMR (500 MHz, 1:1 $CDCl_3/CD_3OD$) δ ppm 3.30 (m, 4 H), 3.94 (m, 4 H), 7.04 (dd, *J* = 8.3, 2.4 Hz, 1 H), 7.31 (m, 1 H), 7.36 (m, 1 H), 7.44 (t, *J* = 8.3 Hz, 1 H), 7.89 (s, 1 H), 7.95 (s, 1 H), 8.14 (m, 1 H), 8.57 (s, 1 H), 8.66 (d, *J* = 2.0 Hz, 1 H), 8.75 (s, 1 H). LCMS found 390.1, $[M+H]^+$.

N2-(6-(3-morpholinophenyl)quinazolin-4-yl)pyridine-2,3-diamine (9t). A flask containing **9r** (0.075 g, 0.170 mmol) was purged with nitrogen three times. To this flask was added a degassed solution of potassium hydroxide (1.573 g, 28.0 mmol) in water (1 mL) and methanol (1 mL). The reaction mixture was heated at 65^{o}C for 12 h. The organic layer was extracted three times with dichloromethane, dried over sodium sulfate and concentrated under reduced pressure. The product was separated by silica column chromatography (dichloromethane/isopropanol) and purified by reverse phase chromatography (water/acetonitrile) to obtain the product in a 59% yield as a yellow solid. ^{1}H NMR (500 MHz, $CDCl_3$) δ ppm 3.26 (m, 4 H), 3.91 (m, 4 H), 4.60 (s, 2 H), 6.84 (dd, *J* = 7.8, 5.4 Hz, 1 H), 6.97 (m, 1 H), 7.03 (dd, *J* = 7.6, 1.7 Hz, 1 H), 7.20 (m, 2 H), 7.40 (t, *J* = 8.3 Hz, 1 H), 7.72 (m, 2 H), 7.88 (dd, *J* = 8.3, 2.4 Hz, 1 H), 8.13 (s, 1 H), 8.67 (d, *J* = 2.0 Hz, 1 H). LCMS found 399.1, $[M+H]^+$.

Reaction Conditions for Nucleotide Library (10a and 10b). In a microwave tube was added **8** (0.039 g, 0.121 mmol), potassium carbonate (0.033 g, 0.242 mmol), and the respective amine (0.121 mmol). The tube was sealed and purged with nitrogen three times. Dry acetone (1 mL) was added under nitrogen and the flask was heated in the microwave at 120^{o}C for 1 h. The reaction mixture was concentrated under reduced pressure, separated by silica column

chromatography (dichloromethane/isopropanol) and purified by reverse phase chromatography (water/acetonitrile) to obtain the product.

4-((6-(3-morpholinophenyl)quinazolin-4-yl)amino)pyrimidin-2(1H)-one (10a). (Yellow solid, Yield: 5%). ^{1}H NMR (500 MHz, DMSO-d_6) δ ppm 3.20 (m, 4 H), 3.77 (m, 4 H), 6.00 (d, *J* = 7.3 Hz, 1 H), 7.04 (dd, *J* = 8.3, 2.0 Hz, 1 H), 7.12 (m, 1 H), 7.23 (m, 1 H), 7.39 (t, *J* = 7.8 Hz, 1 H), 7.60 (m, 1 H), 7.68 (m, 1 H), 7.91 (d, *J* = 7.3 Hz, 1 H), 7.95 (d, *J* = 2.0 Hz, 1 H), 8.17 (d, *J* = 8.8 Hz, 1 H), 8.37 (dd, *J* = 8.8, 2.0 Hz, 1 H), 9.28 (s, 1 H). LCMS found 401.2, $[M+H]^+$.

5-fluoro-4-((6-(3-morpholinophenyl)quinazolin-4-yl)amino)pyrimidin-2(1H)-one (10b). (Pale yellow solid, Yield: 23%). ^{1}H NMR (500 MHz, 1:1 $CDCl_3$/CD_3OD) δ ppm 3.28 (m, 4 H), 3.92 (m, 4 H), 7.05 (dd, *J* = 8.3, 2.4 Hz, 1 H), 7.26 (m, 2 H), 7.43 (t, *J* = 7.8 Hz, 1 H), 8.05 (d, *J* = 2.9 Hz, 1 H), 8.08 (d, *J* = 8.8 Hz, 1 H), 8.27 (dd, *J* = 8.8, 2.4 Hz, 1 H), 8.49 (d, *J* = 2.0 Hz, 1 H), 8.77 (s, 1 H). LCMS found 419.0, $[M+H]^+$.

N-(3-chloro-4-((3-fluorobenzyl)oxy)phenyl)-6-(4,4,5,5-tetramethyl-1,3,2-dioxaborolan-2-yl)quinazolin-4-amine (12). N-(3-chloro-4-((3-fluorobenzyl)oxy)phenyl)-6-iodoquinazolin-4-amine (0.108g, 0.213 mmol), 4,4,4',4',5,5,5',5'-octamethyl-2,2'-bi(1,3,2-dioxaborolane) (0.206g, 0.811 mmol), potassium acetate (0.185g, 1.885 mmol), [1,1'-bis(diphenylphosphino)ferrocene]dichloropalladium(II) dichloromethane adduct (0.022g, 0.027 mmol), and N,N'-dimethylformamide (2.5 mL) were added together and heated at 85^{o}C for 12 h. The reaction mixture was concentrated under reduced pressure and purified by silica column chromatography (hexanes/ethyl acetate) to afford the product in 82% yield as a pale yellow solid. ^{1}H NMR (500 MHz, DMSO-d_6) δ ppm 1.35 (s, 12 H), 5.25 (s, 2 H), 7.15 (td, *J* = 8.8, 2.4 Hz, 1 H), 7.24 (d, *J* = 9.3 Hz, 1 H), 7.32 (m, 2 H), 7.47 (m, 1 H), 7.73 (d, *J* = 8.3 Hz, 1 H), 7.77 (dd, *J*

= 8.8, 2.4 Hz, 1 H), 8.03 (m, 2 H), 8.59 (s, 1 H), 8.87 (s, 1 H), 10.09 (s, 1 H). LCMS found 506.1, $[M+H]^+$.

4-(4-chloropyrimidin-2-yl)morpholine and 4-(2-chloropyrimidin-4-yl)morpholine (17, 18). A solution of 2,4-dichloropyrimidine (0.500 g, 3.36 mmol) and N,N-diisopropylethylamine (0.818 mL, 4.70 mmol) in isopropanol (5 mL) was stirred at 0°C. Morpholine (0.319 mL, 3.69 mmol) was added dropwise and the solution continued to stir at 0°C for 30 mins, and then room temperature for 12 h. The reaction mixture was concentrated under reduced pressure and then partitioned between ethyl acetate and water. The organic layer was extracted three times, washed with brine, dried over sodium sulfate, and concentrated to dryness. The products were purified by silica column chromatography in hexanes and ethyl acetate to afford 4-(4-chloropyrimidin-2-yl)morpholine and 4-(2-chloropyrimidin-4-yl)morpholine in 7% and 92% yields, respectively.

4-(4-chloropyrimidin-2-yl)morpholine (15). (White solid, Yield: 7%). ^{1}H NMR (500 MHz, $CDCl_3$) δ ppm 3.74 (m, 4 H), 3.81 (m, 4 H), 6.53 (d, *J* = 4.9 Hz, 1 H), 8.16 (d, *J* = 4.9 Hz, 1 H). LCMS found 200.0, $[M+H]^+$.

4-(2-chloropyrimidin-4-yl)morpholine (16). (White solid, Yield: 92%). ^{1}H NMR (500 MHz, $CDCl_3$) δ ppm 3.64 (br. s, 4 H), 3.77 (m, 4 H), 6.38 (d, *J* = 5.9 Hz, 1 H), 8.07 (d, *J* = 6.3 Hz, 1 H). LCMS found 200.0, $[M+H]^+$.

Library Conditions for 17 and 18. Compound **12** (0.088 g, 0.173 mmol), a 2 M solution of sodium carbonate (0.520 mL, 1.039 mmol) in water, tetrakis(triphenylphosphine)palladium(0) (0.014 g, 0.012 mmol), dimethoxyethane (2 mL), ethanol (1.3 mL) and the respective morpholine substituted pyrimidine (0.190 mmol) were added together and heated to 85°C for 12 h. The resulting mixture was concentrated under reduced pressure and the product was separated

by silica column chromatography (hexanes/ethyl acetate) and purified by reverse phase chromatography (water/acetonitrile).

N-(3-chloro-4-((3-fluorobenzyl)oxy)phenyl)-6-(4-morpholinopyrimidin-2-yl)quinazolin-4-amine (17). (Yellow solid, Yield: 9%). ^{1}H NMR (500 MHz, DMSO-d_6) δ ppm 3.75 (m, 8 H), 5.27 (s, 2 H), 6.85 (d, *J* = 5.9 Hz, 1 H), 7.19 (td, *J* = 9.3, 2.4 Hz, 1 H), 7.27 (d, *J* = 8.8 Hz, 1 H), 7.33 (m, 2 H), 7.48 (m, 1 H), 7.74 (dd, *J* = 8.8, 2.4 Hz, 1 H), 7.84 (d, *J* = 8.8 Hz, 1 H), 8.02 (d, *J* = 2.4 Hz, 1 H), 8.43 (d, *J* = 5.9 Hz, 1 H), 8.59 (s, 1 H), 8.78 (dd, *J* = 8.8, 1.0 Hz, 1 H), 9.42 (s, 1 H), 10.19 (s, 1 H). LCMS found 543.1, $[M+H]^+$.

N-(3-chloro-4-((3-fluorobenzyl)oxy)phenyl)-6-(2-morpholinopyrimidin-4-yl)quinazolin-4-amine (18). (Yellow solid, Yield: 28%). ^{1}H NMR (500 MHz, DMSO-d_6) δ ppm 3.72 (m, 4 H), 3.85 (m, 4 H), 5.28 (s, 2 H), 7.19 (td, *J* = 8.8, 2.4 Hz, 1 H), 7.32 (m, 3 H), 7.48 (m, 2 H), 7.71 (dd, *J* = 8.8, 2.4 Hz, 1 H), 7.88 (d, *J* = 8.8 Hz, 1 H), 7.99 (d, *J* = 2.9 Hz, 1 H), 8.58 (d, *J* = 4.9 Hz, 1 H), 8.62 (s, 1 H), 8.64 (dd, *J* = 8.8, 2.0 Hz, 1 H), 9.16 (s, 1 H), 10.04 (s, 1 H). LCMS found 543.1, $[M+H]^+$.

2-morpholinoacetamide (20) [29]. (White solid, Yield: 91%). ^{1}H NMR (500 MHz, $CDCl_3$) δ ppm 2.36 (m, 4 H), 2.80 (s, 2 H), 3.52 (m, 4 H), 6.86 (s, 1 H), 6.99 (s, 1 H). GCMS EI: 144.1, $[M]^{\bullet+}$.

N-(4-((3-chloro-4-((3-fluorobenzyl)oxy)phenyl)amino)quinazolin-6-yl)-2-morpholinoacetamide (21) (NEU-1009). A flask with septum containing N-(3-chloro-4-((3-fluorobenzyl)oxy)phenyl)-6-iodoquinazolin-4-amine (0.053 g, 0.104 mmol), **20** (0.015 g, 0.104 mmol), copper(I) iodide (0.020 g, 0.104 mmol), and cesium carbonate (0.068 g, 0.208 mmol) was purged with nitrogen three times. Dry tetrahydrofuran (3 mL) was added and the solution stirred for 5 mins. N,N'-dimethylethylenediamine (0.022 mL, 0.208 mmol) was added to the

solution dropwise and the reaction continued to stir at room temperature for 18 h. The reaction mixture was concentrated under reduced pressure, separated by silica column chromatography (hexanes/ethyl acetate/methanol) and purified by reverse phase chromatography (water/acetonitrile) to obtain a yellow solid in 37% yield. ^{1}H NMR (500 MHz, DMSO-d_6) δ ppm 2.56 (m, 4 H), 3.21 (s, 2 H), 3.67 m, 4 H), 5.25 (s, 2 H), 7.18 (td, *J* = 8.8, 2.4 Hz, 1 H), 7.26 (d, *J* = 8.8 Hz, 1 H), 7.32 (m, 2 H), 7.47 (m, 1 H), 7.70 (dd, *J* = 8.8, 2.4 Hz, 1 H), 7.76 (d, *J* = 8.8 Hz, 1 H), 7.99 (m, 2 H), 8.51 (s, 1 H), 8.61 (d, *J* = 2.0 Hz, 1 H), 9.78 (s, 1 H), 10.01 (s, 1 H). LCMS found 522.1, $[M+H]^+$.

4-(5-bromo-4H-1,2,4-triazol-3-yl)morpholine (22). 3,5-dibromo-4H-1,2,4-triazole (0.174 g, 0.765 mmol), morpholine (0.099 mL, 1.148 mmol), and pyridine (2 ml) in a sealed tube was heated in the microwave at 210°C for 10 mins. The reaction mixture was diluted with ethyl acetate to form a precipitate. The precipitate was collected by vacuum filtration and discarded. The filtrate was concentrated under reduced pressure and purified by reverse phase chromatography (water/acetonitrile) to obtain the product in 52% yield as a yellow solid. ^{1}H NMR (400 MHz, DMSO-d_6) δ ppm 3.26 (m, 4 H), 3.66 (m, 4 H). LCMS found 232.9, $[M+H]^+$.

N-(3-chloro-4-((3-fluorobenzyl)oxy)phenyl)-6-(5-morpholino-4H-1,2,4-triazol-3-yl)quinazolin-4-amine (23) (NEU-2078). (Pale yellow solid, Yield: 5%). **12** (0.137 g, 0.272 mmol), **22** (0.106 g, 0.226 mmol), a 2.0 molar solution of sodium carbonate (0.679 mL, 1.358 mmol) in water, tetrakis(triphenylphosphine)palladium(0) (0.018 g, 0.016 mmol), dimethoxyethane (1 mL), and ethanol (0.7 mL) were added together and heated to 85^{o}C for 12 h. The resulting mixture was concentrated under reduced pressure and the product was separated by silica column chromatography (dichloromethane/isopropanol) and purified by reverse phase chromatography (water/acetonitrile). ^{1}H NMR (500 MHz, 1:1 $CDCl_3$/CD_3OD) δ ppm 3.52 (m, 4

H), 3.85 (m, 4 H), 5.24 (s, 2 H), 7.05 (td, *J* = 8.3, 2.0 Hz, 1 H), 7.15 (d, *J* = 9.3 Hz, 1 H), 7.27 (m, 1 H), 7.32 (m, 1 H), 7.41 (m, 1 H), 7.69 (dd, *J* = 8.8, 2.4 Hz, 1 H), 7.85 (d, *J* = 8.8 Hz, 1 H), 7.99 (d, *J* = 2.4 Hz, 1 H), 8.43 (m, 1 H), 8.60 (s, 1 H), 8.91 (d, *J* = 1.5 Hz, 1 H). LCMS found 532.1, $[M+H]^+$.

6-azido-N-(3-chloro-4-((3-fluorobenzyl)oxy)phenyl)quinazolin-4-amine (13). To a solution of **12** (0.138 g, 0.272 mmol) in methanol (2 mL) was added sodium azide (0.027 g, 0.408 mmol) and copper (II) acetate (0.005 g, 0.027 mmol). The reaction was heated at 55°C for 12 h, concentrated under reduced pressure, and then the product was obtained through column chromatography (hexanes/ethyl acetate) in 88% yield as a reddish-brown solid. ^{1}H NMR (400 MHz, DMSO-d_6) δ ppm 5.26 (s, 2 H), 7.18 (td, *J* = 8.8, 2.2 Hz, 1 H), 7.31 (m, 3 H), 7.47 (m, 1 H), 7.60 (dd, *J* = 8.8, 2.2 Hz, 1 H), 7.71 (dd, *J* = 9.5, 2.9 Hz, 1 H), 7.82 (d, *J* = 8.8, 1 Hz), 7.99 (d, *J* = 2.9 Hz, 1 H), 8.25 (d, *J* = 2.2 Hz, 1 H), 8.55 (s, 1 H), 9.80 (s, 1 H). LCMS found 421.0, $[M+H]^+$.

N-(3-chloro-4-((3-fluorobenzyl)oxy)phenyl)-6-(5-(morpholinomethyl)-1H-1,2,3-triazol-1-yl)quinazolin-4-amine (23) (NEU-2083). In a microwave vial was added **13** (0.073 g, 0.173 mmol) and Cp*RuCl(PPh_3)$_2$ (0.003 g, 0.004 mmol), and then sealed and purged with nitrogen three times. A solution of 4-(prop-2-yn-1-yl)morpholine (0.022 g, 0.173 mmol) in 1.6 mL of anhydrous dioxane was added to the reaction mixture and then heated in the microwave at 150^{o}C for 30 mins. The resulting mixture was concentrated under reduced pressure and the product was separated by silica column chromatography (dichloromethane/isopropanol) and purified by reverse phase chromatography (water/acetonitrile). (Yellow solid, Yield: 13%). ^{1}H NMR (500 MHz, 1:1 $CDCl_3$/CD_3OD) δ ppm 2.48 (m, 4 H), 3.65 (m, 4 H), 3.69 (s, 2 H), 5.21 (s, 2 H), 7.03

(dd, *J* = 8.3, 2.4 Hz, 1 H), 7.09 (d, *J* = 8.8 Hz, 1 H), 7.23 (m, 1 H), 7.28 (m, 1 H), 7.38 (m, 1 H), 7.58 (dd, *J* = 8.8 Hz, 2.4 Hz, 1 H), 7.85 (s, 1 H), 7.87 (d, *J* = 2.9 Hz, 1 H), 7.99 (d, *J* = 8.8 Hz, 1 H), 8.19 (dd, *J* = 9.0, 2.2 Hz, 1 H), 8.66 (s, 1 H). LCMS found 546.1, $[M+H]^+$.

4-(4-bromopyrimidin-2-yl)morpholine and 4-(2-bromopyrimidin-4-yl)morpholine (28a,b) [32]. 2,4-dibromopyrimidine (438.4 mg, 1.84 mmol) and potassium carbonate (1.27 g, 9.21 mmol) in tetrahydrofuran (10 mL) were added together and stirred at room temperature for 5 mins. Morpholine (174.8 µL, 2.03 mmol) was then added dropwise and the solution continued to stir at room temperature for 5 h. The reaction mixture was filtered and the filtrate was collected and then concentrated under reduced pressure. The products were purified by silica column chromatography in hexanes and ethyl acetate to afford **28a** and **28b** in 19% and 66% yields, respectively.

4-(4-bromopyrimidin-2-yl)morpholine (28a). (White solid, Yield: 19%). ^{1}H NMR (500 MHz, $CDCl_3$) δ ppm 3.74 - 3.77 (m, 4 H) 3.79 - 3.83 (m, 4 H) 6.70 (d, *J*=4.88 Hz, 1 H) 8.05 (d, *J*=4.88 Hz, 1 H). LCMS found 246.0, $[M+H]^+$.

4-(2-bromopyrimidin-4-yl)morpholine (28b). (White solid, Yield: 66%) ^{1}H NMR (500 MHz, $CDCl_3$) δ ppm 3.66 (br. s., 4 H) 3.76 - 3.83 (m, 4 H) 6.43 (d, *J*=6.35 Hz, 1 H) 8.02 (d, *J*=6.35 Hz, 1 H). LCMS found 246.0, $[M+H]^+$.

2-amino-5-(4,4,5,5-tetramethyl-1,3,2-dioxaborolan-2-yl)benzonitrile (30). (White solid, Yield: 88%). 2-amino-5-bromobenzonitrile (295.6 mg, 1.5 mmol), 4,4,4',4',5,5,5',5'-octamethyl-2,2'-bi(1,3,2-dioxaborolane) (761.8 mg, 3.0 mmol), [1,1′-bis(diphenylphosphino)ferrocene]dichloropalladium(II), complex with dichloromethane (122.5 mg, 0.15 mmol), and potassium acetate (441.6 mg, 4.5 mmol) were added to a microwave vial and sealed with a stir bar. The vial was vacuum purged with nitrogen 3 times, after which dry,

degassed 1,4-dioxane (11 mL) was added under nitrogen. The reaction mixture was heated in the microwave at 130°C for 1 h. The reaction mixture was filtered through celite, concentrated under reduced pressure, and purified by silica column chromatography (hexanes/ethyl acetate) to afford the product in 82% yield as a white solid. ^{1}H NMR (500 MHz, $CDCl_3$) δ ppm 1.33 (s, 12 H) 4.57 (br. s., 2 H) 6.72 (d, *J*=8.30 Hz, 1 H) 7.73 (d, *J*=8.30 Hz, 1 H) 7.88 (s, 1 H). LCMS found 245.1, $[M+H]^+$.

2-amino-5-(2-morpholinopyrimidin-4-yl)benzonitrile (31a). (White solid, Yield: 53%). **30** (84.8 mg, 0.35 mmol), 4-(4-bromopyrimidin-2-yl)morpholine (93.3 mg, 0.38 mmol), cesium carbonate (339.6 mg, 1.04 mmol), and tetrakis(triphenylphosphine)palladium(0) (28.1 mg, 0.024 mmol) were added to a microwave vial and sealed with a stir bar. The vial was vacuum purged with nitrogen 3 times, after which degassed solution of 1,4-dioxane/water (3:1) (3 mL) was added under nitrogen. The reaction mixture was heated in the microwave at 130°C for 15 mins. The reaction mixture was filtered through celite, concentrated under reduced pressure, and purified by silica column chromatography (hexanes/ethyl acetate) to afford the product in 53% yield as a white solid. ^{1}H NMR (500 MHz, $CDCl_3$) δ ppm 3.77 - 3.86 (m, 4 H) 3.86 - 3.93 (m, 4 H) 4.67 (br. s., 2 H) 6.80 - 6.83 (m, 1 H) 6.84 - 6.87 (m, 1 H) 8.04 (dd, *J*=8.79, 1.95 Hz, 1 H) 8.18 (d, *J*=1.95 Hz, 1 H) 8.32 - 8.38 (m, 1 H). LCMS found 282.1, $[M+H]^+$.

2-amino-5-(4-morpholinopyrimidin-2-yl)benzonitrile (31b). (White solid, Yield: 95%) **30** (200 mg, 0.819 mmol), 4-(2-bromopyrimidin-4-yl)morpholine (220 mg, 0.901 mmol), cesium carbonate (801 mg, 2.46 mmol), and tetrakis(triphenylphosphine)palladium(0) (66.3 mg, 0.057 mmol) were added to a microwave vial and sealed with a stir bar. The vial was vacuum purged with nitrogen 3 times, after which degassed solution of 1,4-dioxane/water (3:1) (3 mL) was added under nitrogen. The reaction mixture was heated in the microwave at 130°C for 10 mins.

The reaction mixture was filtered through celite, concentrated under reduced pressure, and purified by silica column chromatography (hexanes/ethyl acetate) to afford the product in 95% yield as a white solid. ^{1}H NMR (500 MHz, $CDCl_3$) δ ppm 3.72 (d, *J*=4.39 Hz, 4 H) 3.80 - 3.87 (m, 4 H) 4.62 (s, 2 H) 6.38 (d, *J*=6.35 Hz, 1 H) 6.80 (d, *J*=8.79 Hz, 1 H) 8.30 (d, *J*=6.35 Hz, 1 H) 8.38 (dd, *J*=8.55, 1.71 Hz, 1 H) 8.49 (d, *J*=1.46 Hz, 1 H). LCMS found 282.1, $[M+H]^+$.

6-(2-morpholinopyrimidin-4-yl)quinazolin-4-amine (32a) [33]. (Light brown solid, Yield: 78%) **31a** (50 mg, 0.18 mmol) and formamide (0.7 mL) were added to a microwave vial. The reaction mixture was then heated in the microwave at 200°C for 1 h. The product was collected by vacuum filtration as a light brown solid in 78% yield. ^{1}H NMR (500 MHz, DMSO-d_6) δ ppm 3.70 - 3.74 (m, 4 H) 3.84 (t, *J*=4.64 Hz, 4 H) 7.42 (d, *J*=5.37 Hz, 1 H) 7.75 (d, *J*=8.79 Hz, 1 H) 8.43 (s, 1 H) 8.53 (d, *J*=4.88 Hz, 1 H) 8.55 - 8.58 (m, 1 H) 8.97 (d, *J*=1.95 Hz, 1 H). LCMS found 309.0, $[M+H]^+$.

6-(4-morpholinopyrimidin-2-yl)quinazolin-4-amine (32b) [33].(Pale yellow solid, Yield: 84%). **31b** (250 mg, 0.89 mmol) and formamide (1.42 mL) were added to a microwave vial. The reaction mixture was then heated in the microwave at 200°C for 1 h. A pale yellow-tan solid was collected by vacuum filtration and washed with water. The aqueous filtrate was extracted 3 times with ethyl acetate. The combined organic layers were washed with water and brine, collected, dried using sodium sulfate, filtered, and concentrated under reduced pressure. The concentrated organic layer and solid, filtered product were combined and purified by silica column chromatography (dichloromethane/(5% ammonium hydroxide/methanol) to afford the product in 84% yield as a pale yellow solid. ^{1}H NMR (500 MHz, CD_3OD-d_4) δ ppm 3.82 (s, 8 H) 6.73 (d, *J*=5.86 Hz, 1 H) 7.77 (d, *J*=8.79 Hz, 1 H) 8.32 (d, *J*=6.35 Hz, 1 H) 8.40 (s, 1 H) 8.72 (dd, *J*=8.79, 1.95 Hz, 1 H) 9.07 (d, *J*=1.46 Hz, 1 H). LCMS found 309.0, $[M+H]^+$.

6-(2-morpholinopyrimidin-4-yl)-N-(pyrimidin-2-yl)quinazolin-4-amine (NEU-4436) (33a). (Pale yellow solid, Yield: 67%) **32a** (23.2 mg, 0.075 mmol), 2-chloropyrimidine (34.5 mg, 0.30 mmol), sodium *tert*-butoxide (28.9 mg, 0.30 mmol), tris(dibenzylideneacetone)dipalladium(0) (2.1 mg, 0.002 mmol), and 1,1'-bis(diphenylphosphino)ferrocene (5.0 mg, 0.009 mmol) were added to a microwave vial and sealed with a stir bar. The vial was vacuum purged with nitrogen 3 times, after which dry, degassed 1,4-dioxane (1.4 mL) was added under nitrogen. The reaction mixture was heated in the microwave at 170°C for 2 h. The reaction mixture was filtered through celite, concentrated under reduced pressure, and purified by silica column chromatography (dichloromethane/(5% ammonium hydroxide/methanol) to afford the product in 67% yield as a pale yellow solid. ^{1}H NMR (500 MHz, DMSO-d_6) δ ppm 3.70 - 3.74 (m, 4 H) 3.80 - 3.85 (m, 4 H) 7.24 - 7.27 (m, 1 H) 7.54 - 7.56 (m, 1 H) 7.97 - 8.00 (m, 1 H) 8.55 - 8.57 (m, 1 H) 8.69 - 8.73 (m, 1 H) 8.75 - 8.77 (m, 2 H) 8.82 - 8.83 (m, 1 H) 9.20 - 9.22 (m, 1 H) 11.09 - 11.11 (m, 1 H). LCMS found 387.0, $[M+H]^+$.

6-(2-morpholinopyrimidin-4-yl)-N-(pyridin-4-yl)quinazolin-4-amine (NEU-4444) (33b). (Pale yellow solid, Yield: 34%) **32a** (27.0 mg, 0.088 mmol), 4-chloropyridine hydrochloride (52.5 mg, 0.35 mmol), sodium *tert*-butoxide (42.1 mg, 0.44 mmol), tris(dibenzylideneacetone)dipalladium(0) (2.4 mg, 0.003 mmol), and 1,1'-bis(diphenylphosphino)ferrocene (5.8 mg, 0.010 mmol) were added to a microwave vial and sealed with a stir bar. The vial was vacuum purged with nitrogen 3 times, after which dry, degassed 1,4-dioxane (1.0 mL) was added under nitrogen. The reaction mixture was heated in the microwave at 170°C for 1 h. The reaction mixture was filtered through celite, concentrated under reduced pressure, and purified twice by silica column chromatography (dichloromethane/(5% ammonium hydroxide/methanol) to afford the product in 34% yield as a

pale yellow solid. ^{1}H NMR (500 MHz, METHANOL-d_4) δ ppm 3.76 - 3.81 (m, 4 H) 3.86 - 3.92 (m, 4 H) 7.34 (d, *J*=5.37 Hz, 1 H) 7.87 (d, *J*=8.79 Hz, 1 H) 8.06 (d, *J*=5.37 Hz, 2 H) 8.42 - 8.49 (m, 3 H) 8.63 (dd, *J*=8.79, 1.95 Hz, 1 H) 8.73 (s, 1 H) 9.02 (d, *J*=1.46 Hz, 1 H). LCMS found 386.0, $[M+H]^+$.

6-(4-morpholinopyrimidin-2-yl)-N-(pyrimidin-2-yl)quinazolin-4-amine (NEU-4446) (33c). (Pale yellow solid, Yield: 30%) **32b** (50.0 mg, 0.16 mmol), 2-chloropyrimidine (55.7 mg, 0.49 mmol), sodium *tert*-butoxide (93.5 mg, 0.97 mmol), tris(dibenzylideneacetone)dipalladium(0) (4.5 mg, 0.005 mmol), and 1,1'-bis(diphenylphosphino)ferrocene (10.8 mg, 0.019 mmol) were added to a microwave vial and sealed with a stir bar. The vial was vacuum purged with nitrogen 3 times, after which dry, degassed 1,4-dioxane (1.2 mL) was added under nitrogen. The reaction mixture was heated in the microwave at 170°C for 1 h. The reaction mixture was filtered through celite, concentrated under reduced pressure, and purified by silica column chromatography (dichloromethane/(5% ammonium hydroxide/methanol). The product was further purified by silica column chromatography (dichloromethane/(1% ammonium hydroxide/methanol) to afford the product in 30% yield as a pale yellow solid. ^{1}H NMR (500 MHz, METHANOL-d_4) δ ppm 3.69 - 3.86 (m, 8 H) 6.64 (d, *J*=5.86 Hz, 1 H) 7.11 - 7.17 (m, 1 H) 7.74 (br. s., 1 H) 8.22 - 8.29 (m, 1 H) 8.47 (br. s., 1 H) 8.63 - 8.74 (m, 3 H) 9.33 (br. s., 1 H). LCMS found 387.0, $[M+H]^+$.

6-(4-morpholinopyrimidin-2-yl)-N-(pyridin-4-yl)quinazolin-4-amine (NEU-4445) (33d). (Pale yellow solid, Yield: 40%) **32b** (50.0 mg, 0.16 mmol), 4-chloropyridine hydrochloride (24.3 mg, 0.16 mmol), cesium carbonate (211.3 mg, 0.65 mmol), tris(dibenzylideneacetone)dipalladium(0) (4.5 mg, 0.005 mmol), and 1,1'-bis(diphenylphosphino)ferrocene (10.8 mg, 0.019 mmol) were added to a microwave vial and sealed with a stir bar. The vial was vacuum purged with nitrogen 3 times, after which dry,

degassed 1,4-dioxane (1.0 mL) was added under nitrogen. The reaction mixture was heated in the microwave at 170°C for 2 h. The reaction mixture was filtered through celite, concentrated under reduced pressure, and purified by silica column chromatography (dichloromethane/methanol) to afford the product in 40% yield as a pale yellow solid. ^{1}H NMR (500 MHz, DMSO-d_6) δ ppm 3.76 (br. s., 8 H) 6.88 (d, *J*=5.86 Hz, 1 H) 7.94 (d, *J*=8.79 Hz, 1 H) 8.04 (d, *J*=6.35 Hz, 2 H) 8.45 (d, *J*=6.35 Hz, 1 H) 8.51 (d, *J*=6.35 Hz, 2 H) 8.79 (s, 1 H) 8.81 - 8.88 (m, 1 H) 9.51 (d, *J*=1.46 Hz, 1 H) 10.48 (s, 1 H). LCMS found 386.0, $[M+H]^+$.

4.2 Biological assays

The protocols for the biological assays of *Trypanosoma brucei*, *Trypanosoma cruzi*, *Leishmania major* amastigotes and promastigotes, *Plasmodium falciparum* D6, W2, C235, and HepG2 toxicity were performed as previously described [34].

4.3 Computational chemistry

A virtual library of analogs of compound **2** was generated by replacement of the aniline headgroup with commercially available heterocyclic amines downloaded from the Frontier Scientific Website. The structural file containing this virtual library was expanded into a 3D conformer database using *OMEGA* v.2.2.1 (OpenEye Scientific Software, Santa Fe, NM) [37]. allowing an energy window of 8 kcal/mol above ground state, and an msd cutoff of 0.8 Å per the method described in Hawkins *et al.* [38]. In a similar way, a single 3D conformer of **2** was generated. The virtual library conformer library was compared against the 3D conformer of **2** using *ROCS* (OpenEye Scientific Software, Santa Fe, NM). The highest scoring overlaps from *ROCS* were then subjected to electrostatic overlap comparison using *EON* (OpenEye Scientific Software, Santa Fe, NM). After removal of products with an ET_Combo score <1, 121 remaining compounds were filtered by limiting cLog P <3 and TPSA between 60-130 Å (calculated using ChemAxon for Excel). This provided an initial set of nine priority compounds for synthesis (see **Table S.1**).

5. Acknowledgements

Funding from the National Institutes of Health (R56AI099476 to M.P.P. and K.M.-W.), the National Science Foundation (IGERT-NSF-DGE 0965843) and Northeastern University are gratefully acknowledged. We acknowledge ChemAxon and OpenEye Scientific Software for their free academic licenses. We are grateful to AstraZeneca for their computation of ADME properties, and for determination of *in vitro* ADME properties in support of this work.

6. Supporting Information

Data against drug resistant *Plasmodium* strains, and physicochemical property data tables, annotation of compounds with NEU registry numbers and SMILES strings, and biological methods are available. All the data included in this work has also been made available as a publically available data set on www.collaborativedrug.com.

7. References

[1] M.D. Shultz, The thermodynamic basis for the use of lipophilic efficiency (LipE) in enthalpic optimizations, Bioorg Med Chem Lett, (2013).

[2] T.T. Wager, X. Hou, P.R. Verhoest, A. Villalobos, Moving beyond rules: The development of a central nervous system multiparameter optimization (CNS MPO) approach to enable alignment of druglike properties, ACS Chem. Neurosci., 1 (2010) 435-449.

[3] World Health Organization, Human African Trypanosomiasis. World Health Organization Fact Sheet No. 259., in, 2015.

[4] D.M. Klug, M.H. Gelb, M.P. Pollastri, Repurposing strategies for tropical disease drug discovery, Bioorg. Med. Chem. Lett., 26 (2016) 2569-2576.

[5] S.O. Ochiana, N.D. Bland, L. Settimo, R.K. Campbell, M.P. Pollastri, Repurposing human PDE4 inhibitors for neglected tropical diseases. Evaluation of analogs of the human PDE4 inhibitor GSK-256066 as inhibitors of PDEB1 of Trypanosoma brucei, Chem Biol Drug Des, (2014).

[6] E. Amata, N.D. Bland, C.T. Hoyt, L. Settimo, R.K. Campbell, M.P. Pollastri, Repurposing human PDE4 inhibitors for neglected tropical diseases: design, synthesis and evaluation of

cilomilast analogues as *Trypanosoma brucei* PDEB1 inhibitors, Bioorg Med Chem Lett, 24 (2014) 4084-4089.

[7] J.L. Woodring, N.D. Bland, S.O. Ochiana, R.K. Campbell, M.P. Pollastri, Synthesis and assessment of catechol diether compounds as inhibitors of trypanosomal phosphodiesterase B1 (TbrPDEB1), Bioorg. Med. Chem. Lett., 23 (2013) 5971-5974.

[8] N.D. Bland, C. Wang, C. Tallman, A.E. Gustafson, Z. Wang, T.D. Ashton, S.O. Ochiana, G. McAllister, K. Cotter, A.P. Fang, L. Gechijian, N. Garceau, R. Gangurde, R. Ortenberg, M.J. Ondrechen, R.K. Campbell, M.P. Pollastri, Pharmacological validation of *Trypanosoma brucei* phosphodiesterases B1 and B2 as druggable targets for African sleeping sickness, J. Med. Chem., 54 (2011) 8188-8194.

[9] C. Wang, T.D. Ashton, A. Gustafson, N.D. Bland, S.O. Ochiana, R.K. Campbell, M.P. Pollastri, Synthesis and evaluation of human phosphodiesterases (PDE) 5 inhibitor analogs as trypanosomal PDE inhibitors. Part 1. Sildenafil analogs, Bioorg. Med. Chem. Lett., 22 (2012) 2579-2581.

[10] S.O. Ochiana, A. Gustafson, N.D. Bland, C. Wang, M.J. Russo, R.K. Campbell, M.P. Pollastri, Synthesis and evaluation of human phosphodiesterases (PDE) 5 inhibitor analogs as trypanosomal PDE inhibitors. Part 2. Tadalafil analogs, Bioorg. Med. Chem. Lett., 22 (2012) 2582-2584.

[11] R. Diaz-Gonzalez, F.M. Kuhlmann, C. Galan-Rodriguez, L. Madeira da Silva, M. Saldivia, C.E. Karver, A. Rodriguez, S.M. Beverley, M. Navarro, M.P. Pollastri, The susceptibility of trypanosomatid pathogens to PI3/mTOR kinase inhibitors affords a new opportunity for drug repurposing, PLoS Negl Trop Dis, 5 (2011) e1297.

[12] G. Patel, C.E. Karver, R. Behera, P.J. Guyett, C. Sullenberger, P. Edwards, N.E. Roncal, K. Mensa-Wilmot, M.P. Pollastri, Kinase scaffold repurposing for neglected disease drug discovery: discovery of an efficacious, lapatinib-derived lead compound for trypanosomiasis, J. Med. Chem., 56 (2013) 3820-3832.

[13] J.D. Seixas, S.A. Luengo-Arratta, R. Diaz, M. Saldivia, D.I. Rojas-Barros, P. Manzano, S. Gonzalez, M. Berlanga, T.K. Smith, M. Navarro, M.P. Pollastri, Establishment of a structure-activity relationship of 1H-imidazo[4,5-c]quinoline-based kinase inhibitor NVP-BEZ235 as a lead for African sleeping sickness, J. Med. Chem., 57 (2014) 4834-4848.

[14] J.L. Woodring, G. Patel, J. Erath, R. Behera, P.J. Lee, S.E. Leed, A. Rodriguez, R.J. Sciotti, K. Mensa-Wilmot, M.P. Pollastri, Evaluation of Aromatic 6-Substituted Thienopyrimidines as Scaffolds against Parasites That Cause Trypanosomiasis, Leishmaniasis, and Malaria, Medchemcomm, 6 (2015) 339-346.

[15] W.W. Devine, Jennifer; Swaminathan, Uma; Amata, Emanuele; Patel, Gautam; Erath, Jessey; Roncal, Norma; Lee, Patricia; Leed, Susan; Rodriguez, Ana; Mensa-Wilmot, Kojo; Sciotti, Richard; Pollastri, Michael, Protozoan Parasite Growth Inhibitors Discovered by Cross-Screening Yields Potent Scaffolds for Lead Discovery, J. Med. Chem., 58 (2015) 5522-5537.

[16] R. Diaz, S.A. Luengo-Arratta, J.D. Seixas, E. Amata, W. Devine, C. Cordon-Obras, D.I. Rojas-Barros, E. Jimenez, F. Ortega, S. Crouch, G. Colmenarejo, J.M. Fiandor, J.J. Martin, M. Berlanga, S. Gonzalez, P. Manzano, M. Navarro, M.P. Pollastri, Identification and characterization of hundreds of potent and selective inhibitors of Trypanosoma brucei growth from a kinase-targeted library screening campaign, PLoS Negl Trop Dis, 8 (2014) e3253.

[17] S. Katiyar, I. Kufareva, R. Behera, S.M. Thomas, Y. Ogata, M. Pollastri, R. Abagyan, K. Mensa-Wilmot, Lapatinib-binding protein kinases in the African trypanosome: identification of cellular targets for kinase-directed chemical scaffolds, PloS one, 8 (2013) e56150.

[18] R. Behera, S.M. Thomas, K. Mensa-Wilmot, New Chemical Scaffolds for Human African Trypanosomiasis Lead Discovery from a Screen of Tyrosine Kinase Inhibitor Drugs, Antimicrob. Agents Chemother., 58 (2014) 2202-2210.

[19] K. Katsuno, J.N. Burrows, K. Duncan, R. Hooft van Huijsduijnen, T. Kaneko, K. Kita, C.E. Mowbray, D. Schmatz, P. Warner, B.T. Slingsby, Hit and lead criteria in drug discovery for infectious diseases of the developing world, Nat Rev Drug Discov, 14 (2015) 751-758.

[20] S.M. Thomas, A. Purmal, M. Pollastri, K. Mensa-Wilmot, Discovery of a Carbazole-Derived Lead Drug for Human African Trypanosomiasis, Sci. Rep., 6 (2016) 32083.

[21] T.T. Wager, R.Y. Chandrasekaran, X. Hou, M.D. Troutman, P.R. Verhoest, A. Villalobos, Y. Will, Defining desirable central nervous system drug space through the alignment of molecular properties, in vitro ADME, and safety attributes, ACS Chem Neurosci, 1 (2010) 420-434.

[22] H. Chen, S. Winiwarter, M. Fridén, M. Antonsson, O. Engkvist, In silico prediction of unbound brain-to-plasma concentration ratio using machine learning algorithms, J. Mol. Graph. Model., 29 (2011) 985-995.

[23] R. Appel, Tertiary Phosphane-Tetrachloromethane, a Versatile Reagent for Chlorination, Dehydration, and P-N Linkage, Angew. Chem. Int. Edit., 14 (1975) 801-811.

[24] T.H.M. Jonckers, B.U.W. Maes, G.L.F. Lemiere, R. Dommisse, Selective palladium-catalyzed aminations of dichloropyridines, Tetrahedron, 57 (2001) 7027-7034.

[25] J. Kosmrlj, B.U.W. Maes, G.L.F. Lemiere, A. Haemers, The first Pd-catalyzed aminations of 4-chloro-3(2H)-pyridazinones, Synlett, (2000) 1581-1584.

[26] R. Fanelli, A.S. Ressurreicao, L. Dufau, J.L. Soulier, A. Vidu, N. Tonali, G. Bernadat, M. Reboud-Ravaux, S. Ongeri, Introduction of polar groups on the naphthalene scaffold of molecular tongs inhibiting wild-type and mutated HIV-1 protease dimerization, MedChemComm, 5 (2014) 719-727.

[27] K.D. Grimes, A. Gupte, C.C. Aldrich, Copper(II)-Catalyzed Conversion of Aryl/Heteroaryl Boronic Acids, Boronates, and Trifluoroborates into the Corresponding Azides: Substrate Scope and Limitations, Synthesis, 2010 (2010) 1441-1448.

[28] D.M.T. Chan, P.Y.S. Lam, Recent advances in copper-promoted C-heteroatom bond cross-coupling reactions with boronic acids and derivatives, in, Wiley-VCH Verlag GmbH & Co. KGaA, 2005, pp. 205-240.

[29] K.H. Chaudhari, U.S. Mahajan, D.S. Bhalerao, K.G. Akamanchi, Novel and facile transformation of N,N-disubstituted glycylamides into corresponding cyanamides by using pentavalent iodine reagents in combination with tetraethylammonium bromide, Synlett, (2007) 2815-2818.

[30] A.K. Amegadzie, J.P. Beck, K.M. Gardinier, E.J. Hembre, J.C. Ruble, K.A. Savin, B.D. Wakefield, Preparation of Thiazolopyridinones as MCH Receptor Antagonists for Treating and Preventing Symptoms Associated with Obesity and Related Diseases, in, Eli Lilly and Company, USA . 2006, pp. 154 pp.

[31] B.C. Boren, S. Narayan, L.K. Rasmussen, L. Zhang, H. Zhao, Z. Lin, G. Jia, V.V. Fokin, Ruthenium-catalyzed azide-alkyne cycloaddition: scope and mechanism, J Am Chem Soc, 130 (2008) 8923-8930.

[32] K. Singh, H. Kaur, P. Smith, C. de Kock, K. Chibale, J. Balzarini, Quinoline–Pyrimidine Hybrids: Synthesis, Antiplasmodial Activity, SAR, and Mode of Action Studies, J. Med. Chem., 57 (2014) 435-448.

[33] Y. Loidreau, T. Besson, Microwave-assisted thermal decomposition of formamide: a tool for coupling a pyrimidine ring with an aromatic partner, Tetrahedron, 67 (2011) 4852-4857.

[34] G. Patel, N.E. Roncal, P.J. Lee, S.E. Leed, J. Erath, A. Rodriguez, R.J. Sciotti, M.P. Pollastri, Repurposing human Aurora kinase inhibitors as leads for anti-protozoan drug discovery, MedChemComm, 5 (2014) 655-658.

[35] S. Khare, A.S. Nagle, A. Biggart, Y.H. Lai, F. Liang, L.C. Davis, S.W. Barnes, C.J. Mathison, E. Myburgh, M.Y. Gao, J.R. Gillespie, X. Liu, J.L. Tan, M. Stinson, I.C. Rivera, J. Ballard, V. Yeh, T. Groessl, G. Federe, H.X. Koh, J.D. Venable, B. Bursulaya, M. Shapiro, P.K. Mishra, G. Spraggon, A. Brock, J.C. Mottram, F.S. Buckner, S.P. Rao, B.G. Wen, J.R. Walker, T. Tuntland, V. Molteni, R.J. Glynne, F. Supek, Proteasome inhibition for treatment of leishmaniasis, Chagas disease and sleeping sickness, Nature, 537 (2016) 229-233.

[36] I. Torrini, G.P. Zecchini, F. Agrosi, M.P. Paradisi, Applications of 1-alkoxycarbonyl- and 1-acyl-v-triazolo[4,5-b]pyridines as acylating reagents, J. Heterocycl. Chem., 23 (1986) 1459-1463.

[37] P.C. Hawkins, A.G. Skillman, G.L. Warren, B.A. Ellingson, M.T. Stahl, Conformer generation with OMEGA: algorithm and validation using high quality structures from the Protein Databank and Cambridge Structural Database, J Chem Inf Model, 50 (2010) 572-584.

[38] P.C.D. Hawkins, A.G. Skillman, A. Nicholls, Comparison of shape-matching and docking as virtual screening tools., J. Med. Chem., 50 (2007) 74-82.

Highlights:

- 4-Anilinoquinazoline-derived inhibitors of *Trypanosoma brucei* proliferation were redesigned for improved properties, such as LogP, LLE, MPO score
- Replacement of the large, lipophililc headgroup with small aromatic amines provided compounds with improvements in properties
- Various bioisosteric replacements were made for phenyl ring in tail region of molecule
- All compounds were tested against other protozoan pathogens, such a *Trypanosoma cruzi, Leishmania major,* and *Plasmodium falciparum*